9-2010

Experimental Models of Brain Hemorrhage Using Clostridial Collagenase

Tim Lekic

LOMA LINDA UNIVERSITY
School of Medicine
In conjunction with the
Faculty of Graduate Studies

Experimental models of Brain Hemorrhage using *Clostridial* Collagenase

by

Tim Lekic

A Dissertation submitted in partial satisfaction of
the requirements for the degree
Doctor of Philosophy in Physiology

September 2010

Each person whose signature appears below certifies that this dissertation in his/her opinion is adequate, in scope and quality, as a dissertation for the degree Doctor of Philosophy.

_____, Chairperson

John Zhang, Vice Chair, Basic Sciences, Physiology Division, and Professor of Basic Sciences, Neurosurgery, Physiology, Anesthesiology, Neurology, Pathology and Human Anatomy

_____

Richard Hartman, Associate Professor of Psychology

_____

Andre Obenaus, Associate Professor of Radiation Medicine, Biophysics and Bioengineering, Pediatrics, and Radiology

_____

Robert Ostrowski, Assistant Research Professor of Physiology

_____

Jiping Tang, Professor of Physiology

ACKNOWLEDGEMENTS

I would like to express my deepest gratitude and greatest appreciation to my mentor, P.I., and boss, Dr John H. Zhang, for the invaluable support, guidance, inspiration, and teaching, given to me over the years. Dr Zhang, your instruction has taught me the skills needed to overcome any obstacle in life, to answer any question from a colleague, and to uncover the most hidden secrets of science. I am marveled how each day teaches something about leadership, designing a study, writing a paper, preparing a grant. Sir, you model to me what can be the greatest potential for the individual who works hard, and gives so much for helping others, thank you.

To my committee other members, Richard Hartman, Andre Obenaus, Robert Ostrowski, and Jiping Tang, would like to express my appreciation. Rich, thank you for providing all the accommodation and guidance with neurobehavior. Dr Obenaus, for your help and advice, that went above and beyond, with the imaging and review paper. Bob thank you, for your help with study design and reviewing/ editing papers. Dr Tang, I am very grateful for your leadership with the ICH studies.

To my mother, Nada, father, Mike, and sister, Tina Lekic, thank you, for the love and support that sustained me throughout these years. I will give the Chief Acknowledgment to God, who has blessed me with the opportunity and ability to humbly serve others every day, and to complete this great mile-stone. Thank-You.

CONTENTS

TABLES

Tables Page

FIGURES

Figures Page

ABBREVIATIONS

AICA	anterior inferior cerebellar artery
ACA	anterior cerebral artery
ASA	anterior spinal artery
BA	basilar artery
CA	carotid artery
Cb	cerebellum
CCA	common carotid artery
Ctx	cortex
GMH	Germinal Matrix Hemorrhage
ICH	Intracerebral Hemorrhage
MCA	middle cerebral artery
MAP	mean arterial pressure
MMP	matrix metalloproteinase
PCA	posterior cerebral artery
PComA	posterior communicating artery
PICA	posterior inferior cerebellar artery
SCA	superior cerebellar artery
VA	vertebral artery
ZO-1	zona occludens-1

ABSTRACT OF THE DISSERTATION

Experimental models of Brain Hemorrhage using *Clostridial* Collagenase

by

Tim Lekic

Doctor of Philosophy, Graduate Program in Physiology
Loma Linda University, September 2010
Dr John H. Zhang, Chairperson

Stroke is the third leading cause of death and is the leading cause of disability in the United States, and the most severe form is known as intracerebral hemorrhage, which is bleeding into the brain. The goal of this study is to establish novel animal models to buildup foundations for translational research of intracerebral hemorrhage. We, for the first time, established four animal models, including cerebellum hemorrhage, pontine hemorrhage, neonatal matrix hemorrhage and maternal postpartum hemorrhage. Those models are established according to intracerebral hemorrhage patient subpopulations, and characterized the neurobehavioral and morphological outcomes. These studies have established the requisite for future translational work to test neuroprotective drugs with the aim of improving the quality of life for these vulnerable patient populations.

CHAPTER ONE

BACKGROUND

Introduction

The posterior circulation is an understudied brain region that is affected by stroke. When translational research progresses to clinical trials, most trials will enroll very few or completely exclude posterior stroke patients (Clark et al., 2000; Clark et al., 1999; Foulkes et al., 1988; Hacke et al., 1995; Mendelow and Unterberg, 2007). Though posterior circulation strokes are too uncommon in some population centers to achieve sufficient numbers, others try to control for the heterogeneity between the anterior and posterior circulations (Macleod, 2006; Macleod et al., 2005). This leads to evidence-based guidelines that may not sufficiently represent some important spectrums of stroke. For these reasons, experimental animal models could be a useful tool to address posterior circulation treatment strategies (Macleod, 2006). Therefore, this chapter will describe the characteristics of posterior circulation strokes, posterior fossa imaging, neurovascular features, and experimental models for further study of this brain region.

Anatomy of Human Posterior Circulation

Vertebrobasilar Vascular Anatomy

The posterior circulation originates from the paired vertebral arteries and a single basilar artery (Fig. 1A), which supplies the inferior thalamus, occipital lobes, midbrain, cerebellum and brainstem (Fig. 1B-C). At the ponto-medullary junction, the vertebral arteries fuse to form the basilar artery, which then courses along the ventral aspect of the pons and mesencephalon (Duvemoy, 1999). From the basilar artery, dorsolateral (circumferential) superficial vessels branch out to the lateral sides and course toward the cerebellum, while deep (paramedian) branches perforate directly into the brainstem, along the ventral aspect. The basilar artery terminates at the mesencephalic cistern, with perforator branches to parts of the diencephalon, and bifurcation into the paired posterior cerebral arteries (PCA). The PCAs course laterally to combine with the posterior communicating arteries (PComA), and then continue to supply parts of the occipital and temporal cortices.

The circumferential, paramedian and other perforator branches are called “terminal vascular branches”, which lack collateral flow and may potentiate focal ischemia during vertebrobasilar vessel occlusions. The pontine paramedian and the lateral cerebellar circumferential branches are the most common sites of hemorrhage in this brain region. Several clinical syndromes (Table 1) are described for posterior circulation vascular injuries (Ferbert et al., 1990; Worthley and Holt, 2000)**.**

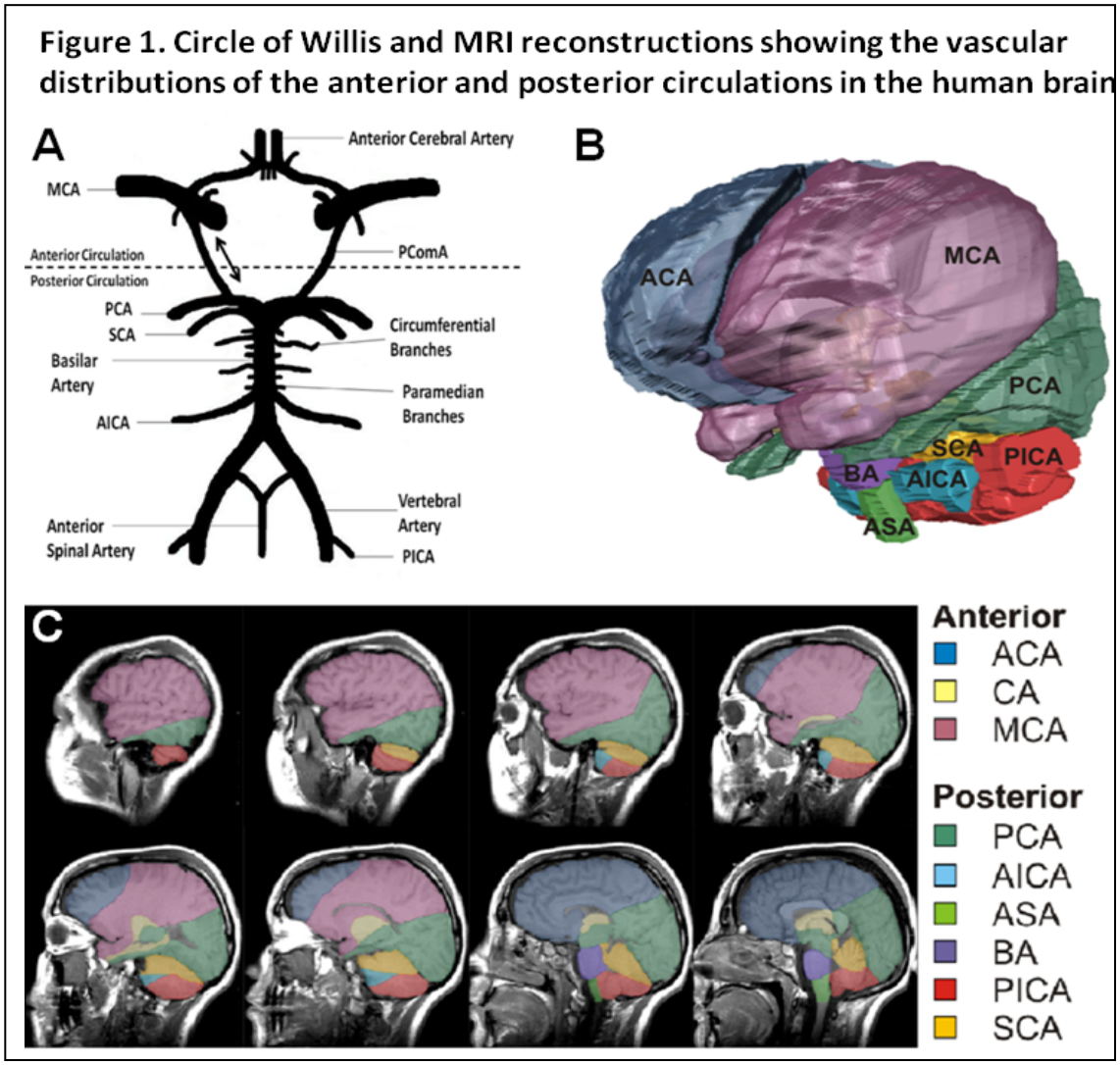

Figure 1. (A) The circle of Willis supplies abundant collateral circulation to the forebrain and hindbrain. *Dotted line* depicts separation between anterior and posterior circulations at the posterior communicating artery (PComA). *Double-headed arrow* indicates potential reversal of flow across PComA. (B) Volumetric 3-dimensional (3D) reconstruction of the human brain is color coded to display the predominant vascular distributions. (C) Serial sagittal sections of (B), showing the depth of anterior and posterior circulations. ACA indicates anterior cerebral artery; CA, carotid artery; MCA, middle cerebral artery; PCA, posterior cerebral artery; AICA, anterior inferior cerebellar artery; ASA, anterior spinal artery; BA, basilar artery; PICA, posterior inferior cerebellar artery; SCA, superior cerebellar artery

The Circle of Willis and Vertebrobasilar Vascular Reserve

Vascular reserve within the basilar circulation includes bidirectional flow through the AICA, PICA and cerebellar leptomeninges (de Oliveira et al., 1995; Lister et al., 1982). The leptomeningeal interconnections between cerebellar arteries are similar to the cerebral-pial network and can reverse blood flow back through the tributaries of the basilar artery (Bergui et al., 2007).

Table 1. Posterior circulation brain regions and clinical signs after injury

Vessel(s)	Brain Region(s)	Contralateral Sign(s)	Ipsilateral Sign(s)
SCA	Superior and middle cerebellar peduncles	Horner's syndrome, Loss of pain and temperature sensation, Nausea, Vomiting	Cerebellar ataxia, Dysarthria, Nausea, Vomiting
AICA	Middle cerebellar peduncle, Pons (lateral-caudal), Caudal Medulla	Loss of pain and temperature sensation, Nausea, Vomiting	Horner's syndrome, Facial and lateral gaze weakness, Deafness, Tinnitus, Nausea, Vomiting
BA (caudal)	Medulla (medial)	Hemipalagia, but facial structures unaffected	Tongue paralysis (hypoglossal nerve)
PICA	Cerebellum (inferior), Medulla (lateral)	Loss of pain and temperature sensation, Nausea, Vomiting	Horner's syndrome, Sensory loss, Diplopia, Nystagmus, Hiccups, Nausea, Vomiting

SCA indicates superior cerebellar artery; AICA, anterior inferior cerebellar artery; BA, basilar artery; PICA, posterior inferior cerebellar artery

Outside the posterior circulation, the direction of blood flow can be reversed through hemodynamic connections between PComA (posterior communicating artery), first PCA segment, and carotid circulation (Bergui et al., 2007). Increased PComA vessel luminal size is directly proportional to improved patient outcome after basilar artery and first segmental PCA occlusions (Steinberg et al., 1993). Patients with PComAs greater than 1 mm in diameter have less ischemic injury during carotid territory occlusions (Schomer et al., 1994). During basilar artery occlusion, PComAs reverse blood flow through the basilar bifurcation, PCA and SCA (quadrigeminal plate) (Bergui et al., 2007). However, individual variations in arterial anatomy and the collateral circulation are common (asymmetric or single vertebral arteries, SCA and AICA branching variants, small PComAs) and these can narrow the basilar artery, diminishing vascular reserve, and leading to a greater incidence and severity of stroke (Bergui et al., 2007; Chaturvedi et al., 1999; Ganesan et al., 2002; Schomer et al., 1994; Steinberg et al., 1993).

Posterior Circulation Stroke

Ischemic Stroke

One quarter of all ischemic strokes are located in the vertebrobasilar (VB) territory (Bamford et al., 1991; Bogousslavsky et al., 1988). These are usually caused by thrombi/emboli, and rarely from vertebral artery dissection of C1-2 vertebral level trauma (Worthley and Holt, 2000). Patients with large vessel (basilar artery or intracranial VA) occlusions affecting the brainstem tend to have

a worse prognosis while small lacunar occlusions generally do well, so long as cardiorespiratory centers are intact (Macleod, 2006). Clinical features are summarized in table 1.

Patient outcomes after VB ischemic stroke have been somewhat the subject of debate. The Oxfordshire Community Stroke Project (Bamford et al., 1991) prospectively followed 129 patients and found a 14% mortality and 18% major disability rate, while the New England Medical Centre Posterior Circulation Registry (NEMC- PCR) (Glass et al., 2002) found a 4% death and 18% disability rate, with a prospective study of 407 patients. For basilar artery occlusion (BAO), the most severe form of VB ischemic stroke, a systematic analysis of 10 published case series and 344 patients, reported an overall death or dependency rate of 76% (Lindsberg and Mattle, 2006), while the NEMC- PCR study with 87 patients reported poor outcomes in 28-58% of patients (Voetsch et al., 2004). Experimental models are available to study ischemic posterior circulation stroke (Table 2).

Table 2. Experimental animal models of posterior circulation stroke

Study	*Stroke Type*	*Species*	*Experimental Method*	*Injury Region*
Henninger *et al,* 2006	Ischemic	Rat	Injected Autologous clots into VA	Brainstem Cerebellum
Shiroyama *et al,* 1991	Ischemic	Rat	Endoluminal suture into BA	Brainstem
Sekiguchi *et al,* 2005	Ischemic	Rat	Microspheres into right CCA	Cerebellum (minor) Forebrain (major)
Yao *et al,* 1990	Ischemic	Rat	Cauterized VA and decreased MAP	Brainstem Cerebellum
Wojak *et al,* 1991	Ischemic	Rat	Coagulated BA	Brain Stem
Cossu *et al,* 1994	Hemorrhagic	Rat	Autologous blood injection	Cerebellum
Hata *et al,* 1994	Ischemic	Cat	Extra-cranial VA occlusion	Brainstem Cerebellum
Nakahara *et al,* 1991	Ischemic	Cat	Radiographic embolization of VA	Brainstem Cerebellum
Chung *et al,* 1993	Hemorrhagic	Cat	Autologous blood injection	Brain Stem
Kuwabara *et al,* 1988	Ischemic	Dog	Occluded perforators of PCA	Brainstem
Guo *et al,* 1995	Ischemic	Dog	Embolized PComA and SCA, then clamped VA and ventral spinal artery	Brainstem
Qureshi *et al,* 2004	Ischemic	Dog	Radiographic embolization BA	Brainstem
Yamada *et al,* 1984	Ischemic	Gerbil	Vascular-clip to BA	Brainstem Cerebellum

VA indicates vertebral artery; BA, basilar artery; CCA, common carotid artery; MAP, mean arterial pressure; PCA, posterior cerebral artery; PComA, posterior communicating artery; SCA, superior cerebellar artery

Intracerebral Hemorrhage

A fifth of all intracerebral hemorrhage (ICH) occurs in the cerebellum or brainstem (Flaherty et al., 2005; Sutherland and Auer, 2006). Brainstem hemorrhages have a 65% mortality rate and around 40% after cerebellar hemorrhage (Balci et al., 2005; Flaherty et al., 2006; Hill et al., 2000). Prolonged endovascular cerebrovascular damage from uncontrolled hypertension leads to arteriosclerotic and amyloid angiopathic changes, vessel fragility and rupture at the deep cerebellar vessels or brainstem basilar (paramedian) branches or at (Qureshi et al., 2001; Sutherland and Auer, 2006). Less common causes of occurrence are: cancer, coagulopathy, or vascular anomalies (arterial-venous malformations, aneurysms, cavernomas and dural arteriovenous fistulas) (Qureshi et al., 2001; Sutherland and Auer, 2006). For most patients, supportive care is the only treatment rendered, since surgery is only available for one-quarter of hospitalized cerebellar hemorrhage patients, and the brainstem is not surgically accessible (Adeoye et al., 2008; Fewel et al., 2003; Morioka et al., 2006; Tuhrim, 2008). Mechanisms of infratentorial hemorrhage have never been studied and to this end we have developed a novel animal model using collagenase to induce hemorrhage (Fig. 2).

Figure 2. Multi-modal MRI and volumetric 3-dimensional (3D) reconstruction of cerebellar and pontine ICH in a rat

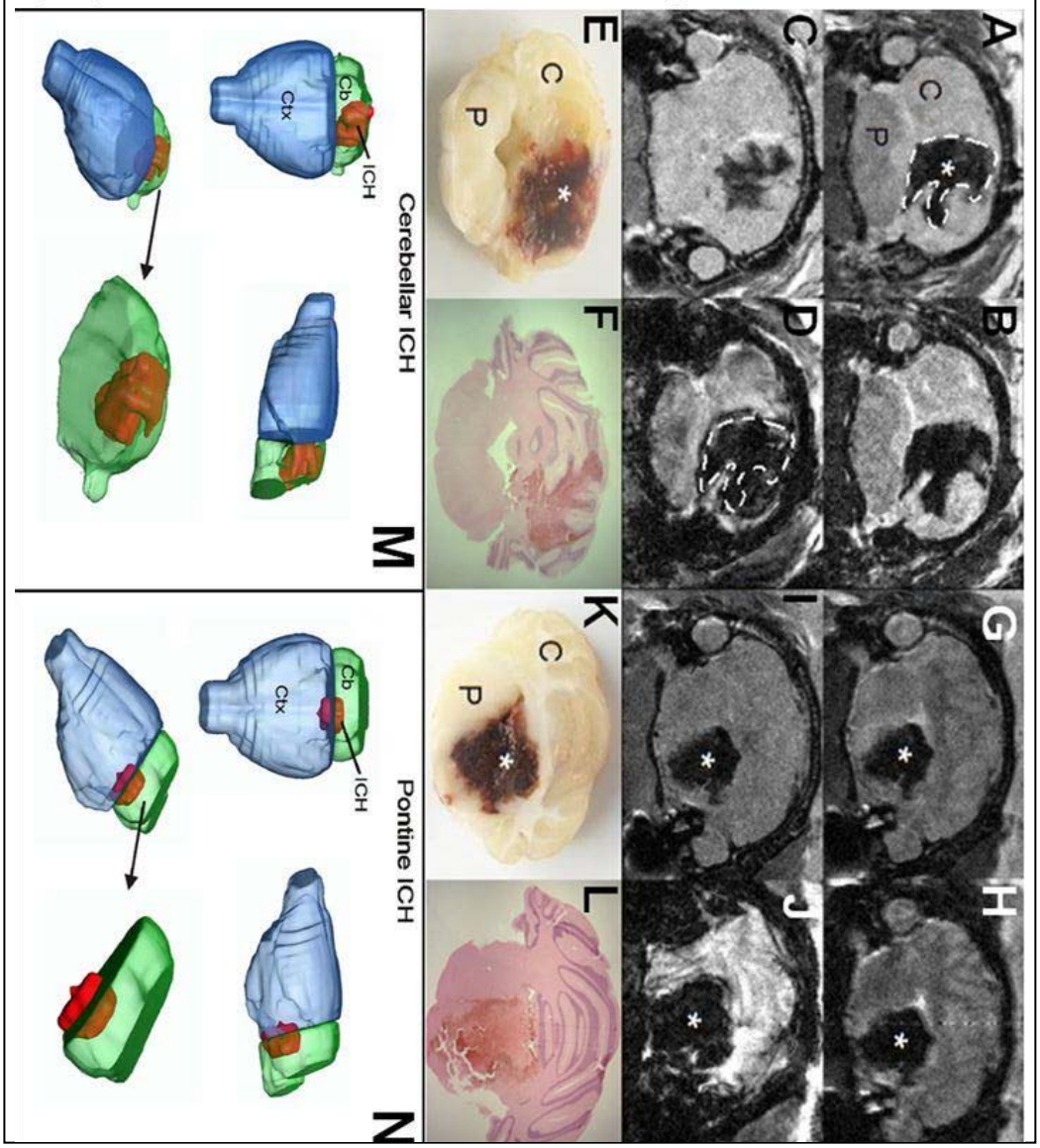

Figure 2. Multiple image contrasts can be used to identify the rostral-caudal extent of ICH (*). (A and G) T2 weighted imaging (T2WI) can easily identify the location of the ICH injury based on loss of signal within the hemorrhage. (B and H) Diffusion-weighted imaging (DWI) is more useful to evaluate ongoing cellular changes within the tissue, with increased signal around the ICH lesion, consistent with cellular swelling. (C and I) T1 weighted imaging (T1WI) evaluates the blood brain barrier by application of an exogenous contrast agent, like Gadolinium. (D and J) More recently susceptibility weighted imaging (SWI) has been shown to be extraordinarily sensitive to extravascular blood (dotted line), SWI identifies a larger region of hemorrhage and is particularly useful for small hemorrhages that may not be visible on standard imaging modalities. All imaging data can be readily correlated with (E and K) gross and (F and L) microscopic histological specimens. (M and N) 3D views of the lesion location and extract quantitative volumetric data simultaneously. Dorsal, saggital and oblique views clearly illustrate the location and size of infratentorial ICH. (For MRI, histological and gross sections: C-cerebellum, P-pons. 3D-reconstructions: Cb-cerebellum, Ctx –cortex).

Diagnostic Imaging of the Posterior Fossa

There are a variety of non-invasive imaging methods that can assess the location and severity of infratentorial stroke, including ultrasound, magnetic resonance imaging (MRI), computed tomography (CT) and positron emission tomography (PET). Duplex transcranial Doppler ultrasound can demonstrate hypoperfusion deficits along the circle of Willis, detecting compromised (collateral) blood flow throughout the vertebrobasilar territory. Ultrasound can also confirm post-treatment recanalizations of hypoperfused vessels (Worthley and Holt, 2000). The current standard for initial assessment of stroke is CT, due to its speed of acquisition and its availability in emergency departments. CT can readily visualize posterior fossa extra-vascular blood either as bleeding from spontaneous intracerebral hemorrhage or hemorrhagic transformation after ischemic stroke, and is commonly used to stratify patients at risk of bleeding prior to anticoagulant or thrombolytic therapy (Donnan, 1992; Worthley and Holt, 2000). While CT is excellent for extravascular blood (and its degradation byproducts) it poorly detects ischemic lesions in the posterior fossa due to the abundance of bony artifacts, except for cerebellar infarctions, which are less obstructed (Donnan, 1992).

In contrast to CT, MRI can easily report both extravascular blood and ischemic tissues throughout the complete hindbrain and posterior fossa (1989). A unique feature of MRI is that multiple contrast levels (e.g. T2, T1, diffusion etc; Fig. 2) are available to ascertain tissue status, including ischemia. Extravascular blood from intracerebral hemorrhage is readily visible on T2-weighted imaging

due to the dephasing properties of heme in the blood. MR imaging of iron within the brain, either as part of hemoglobin or other nonheme-containing regions, has been studied extensively and has recently been reviewed (Haacke et al., 2005). MR and biochemical studies have shown that hemosiderin (proteolytic degradation of ferritin) is likely the MR visible degradation product after hemorrhage (Atlas and Thulbom, 2002; Atlas and Thulborn, 1998; Haque et al., 2003).

MRI is capable of distinguishing at least five distinct intracerebral hemorrhage stages (Atlas and Thulbom, 2002; Bradley, 1993). (1) In the hyperacute phase, intracellular oxyhemoglobin is present (long T1, long T2). (2) Somewhat later, local tissue deoxygenation causes its conversion to deoxyhemoglobin (long T1, short T2). (3) The latter is then denatured over several days to intracellular methemoglobin as heme-iron is oxidized from its ferrous (Fe^{2+}) to ferric (Fe^{3+}) form (short T1, short T2). (4) This transition encourages the loss of heme from hemoglobin (extracellular-methemoglobin, short T1, long T2). After being released, heme molecules are bound extracellularly, transported into cells, and metabolized by heme-oxygenase (HO) (Atlas and Thulbom, 2002; Sung et al., 2000; Wagner et al., 2003). (5) After several days, hemosiderin, a stable pigment composed of ferritin micelles, is formed as a result of macrophage ingestion of hemoglobin (short T2) (Bradley, 1993). In a double injection rodent model of intracerebral hemorrhage into the stiatum, others were able to describe with T2 the temporal time course of these

stages, where stage 1 was present at 0–6 h; stages 2 and 3 at 24–72 h; and stage 5 at 7 days (Belayev et al., 2007).

More recently, susceptibility weighted MR imaging (SWI) has shown promise to visualize and quantify tissue iron in the brain. Clinically, SWI has been used to diagnose neurotrauma (Tong et al., 2004), stroke (Hermier and Nighoghossian, 2004; Wycliffe et al., 2004), tumors (Haacke et al., 2002), and the development of intracerebral hemorrhage in stroke patients (Greer et al., 2004). SWI images appear to have a larger area of susceptibility than that seen on T2-weighted images, due in part to the large phase differences between normal tissue and the injected blood in the intracerebral hemorrhage (Atlas and Thulbom, 2002; Haacke et al., 2005).

Pathophysiology of Posterior Circulation

Vascular Responses to Stroke

Similar mechanisms are shared between ischemic and hemorrhagic strokes (Xi et al., 2006). In the brain, cerebrovascular autoregulation maintains optimal tissue perfusion by constricting or dilating the arterial system in response to wide variations of systemic pressure (MABP) and local levels of CO_2 (Kety and Schmidt, 1948). Stroke leads to damaged cerebral autoregulation capacity and a greater dependence upon systemic arterial pressure (Dawson et al., 2003; Eames et al., 2002; Schwarz et al., 2002). This occurs after both carotid and vertebrobasilar-based ischemic strokes (Dawson et al., 2000; Dawson et al., 2003). Impaired autoregulation has been recognized as an important mechanism

of secondary brain injury and edema formation in patients after ischemic stroke (Dohmen et al., 2007) and intracerebral hemorrhage (Diedler et al., 2009). For this reason, MABP and respiration rate are closely controlled at intensive care units.

The vertebrobasilar vessels have a greater capacity to mechanically vasodilate and vasoconstrict compared to the MCA, suggesting greater dynamic autoregulatory ability (Hida et al., 1996; Ito et al., 2000; Reinhard et al., 2008). This may enable the hindbrain to divert blood flow to the carotid system during cerebrovascular strain, since a drop in CNS perfusion leads to a proportionally greater diminished flow across the BA compared to the MCA (Garbin et al., 1997). Systemic CO_2 and MABP changes superimposed upon permanent PCA occlusion in dogs showed graded autoregulatory decompensation caudally from the supratentorium to the brainstem, while the MCA autoregulation was preserved (Matsumoto et al., 2000). Experimental work in rats showed cerebral sparing when systemic hypotension led to progressive declines of cerebellar autoregulatory kinetics while MCA autoregulatory kinetics remain intact (Merzeau et al., 2000). Cerebellar autoregulatory impairment also occurred after bilateral carotid ligation in spontaneously hypertensive rats (Shiokawa et al., 1988). In opposition, the addition of hypocapnia to systemic hypotension in cats, led to greater ischemic susceptibility in the MCA-region compared to the cerebellum (Sato et al., 1984). Therefore cerebellar autoregulatory kinetics may handle CO_2 changes more favorably in the face of hypoperfusion, while a drop in MABP

without systemic CO_2 changes would affect the cerebellum more severely (Merzeau et al., 2000).

The cerebellum and brainstem have an abundance of white matter tracts. Magnetic resonance imaging (MRI) perfusion and diffusion studies in humans have determined white matter to have an infarction threshold of 20ml/100g/minute, while gray matter can sustain flow down to infarctions starting at 12ml/100g/minute (Bristow et al., 2005). A greater density of white matter tracts in the hindbrain would imply greater vulnerability to ischemic injury. The viability of brainstem cardiorespiratory centers during periods of severe systemic hypotension, global cerebral ischemia and cardiac arrest deserve further study.

Neural Consequences from Stroke

Ischemic interruption of cerebral blood flow leads to hypoxic and anoxic brain injury, increased neuronal excitability, and cell death (Fujiwara et al., 1987). Reperfusion following cerebrovascular ischemia augments this injury through free radial production and mitochondrial dysfunction (Back, 1998; Facchinetti et al., 1998). Similar mechanisms are at play after hemorrhagic stroke also (Xi et al., 2006). The cells comprising the CA1 hippocampal region are known for their vulnerability to ischemia, but these cells may be more resistant than several areas of the hindbrain (Donnelly et al., 1992; Hata et al., 1993). Electrophysiological studies after hypoxic injury have shown greater neuronal excitability in the hypoglossal (CNXII) and dorsal vagal motor (DVMN) cranial nuclei of the brainstem compared to hippocampal CA1 regions (Donnelly et al.,

1992). After anoxia, the hypoglossal nucleus has shown both greater initial injury, and also impaired recovery as compared to temporal lobe neurons (O'Reilly et al., 1995). In-vitro simulation of ischemic reperfusion injury, using cell cultures of oxygen-glucose deprivation followed by re- oxygenation (OGD-R) showed greater free-radical injury (lipid peroxidation) and mitochondrial impairment in cerebellar cells compared to cerebral cortical cell culture (Scorziello et al., 2001).

Comparing cerebellar to brainstem injury after vertebral arterial occlusion, in gerbils (experimental models are summarized in Table 2), showed that the greatest amount of cell death were near areas of coordination and balance (cerebellar interpositus and lateral vestibular nuclei), while the brainstem cardio-respiratory areas remained relatively intact (Hata et al., 1993). Due to the scattered nature of brainstem nuclei, it is unlikely this finding simply represents re-distribution of blood flow, and deserves further study.

Experimental Animal Models of Posterior Circulation

Animal Studies

Experimental models of posterior circulation stroke have revealed several mechanisms of injury as targets for future study (Table 2). In progressive hypotension in rats, the autoregulatory kinetics remained intact at the cerebrum, while there was a progressive loss of autoregulatory efficacy in the cerebellum (Merzeau et al., 2000). However, a manipulation of both mean arterial blood pressure (MABP) and CO2 levels (in cats) and measuring blood flow (hydrogen

clearance method) in the cerebrum, cerebellum and spinal cord, found a greater susceptibility to pressure dependant ischemia in the cerebrum and spinal cord than the cerebellum, which was relatively resistant (Sato et al., 1984).

De Bray *et al* (de Bray et al., 1994) used transcranial Doppler to compare blood flow in the supratentorial and infratentorial compartments under increasing intracranial pressure (in rabbits). The maximum amplitude of vasomotor activity occurred 30 seconds later in the basilar artery compared to the carotid siphon. This indicates a delayed effect of intracranial pressure on hindbrain microvascular tone. Matsumoto *et al* (Matsumoto et al., 2000) caused permanent occlusion of posterior cerebral artery perforators (canine model). They monitored cerebral blood flow (autoregulation) and carbon dioxide reactivity in response to induced hypotension or hypertension during the occlusion. The cerebral cortex maintained autoregulation and carbon dioxide reactivity, while thalamic autoregulation was maintained during hypotension, but not hypertension. On the other hand, the midbrain had markedly impaired autoregulation and carbon dioxide reactivity. This suggests a differential vulnerability to permanent vascular occlusion, and the brainstem may decompensate compared to the forebrain areas, in spite of abundant posterior collateral circulation.

Using a model of bilateral carotid ligation (in spontaneously hypertensive rats), impaired autoregulation was demonstrated in the cerebrum (Shiokawa et al., 1986). However, the addition of stepwise drop in blood pressure caused impairment of cerebellar autoregulation as well. This suggests a vulnerability to hypotension in a distant area from the original stroke location, an effect possibly

modulated by the alpha-adrenoceptor system (vasoconstrictive), secondary to cerebral hypertensive stimuli or other transtentorial signals (Shiokawa et al., 1988). The chronic collateral vascular response may be age dependant, since bilateral carotid occlusion led to a greater dependence on basilar flow in adult rats, compared to extra-cerebral midline collaterals in the younger animals (Choy et al., 2006).

Many animal studies of anterior circulation ischemic stroke have demonstrated impaired autoregulation after ischemic stroke. The extent of which would depend on occlusion duration and extent of reperfusion hyperemia (Cipolla et al., 1997; Drummond et al., 1989; Olah et al., 2000). This physiological response would be expected to contribute to injury in the posterior brain region also, and needs further study.

New Experimental Models of Hemorrhage

Figure 2 demonstrates novel experimental models of infratentorial intracerebral hemorrhage using clostridial collagenase to induce a hematoma in the cerebellum or brainstem. These are the first experimental models to successfully mimic the clinical hemorrhage at the infratentorial region. In agreement with the clinical picture, these animals were highly ataxic, with motor-sensory, cognitive, and cranial nerve deficits that recovered over time. Most animals survived past 30 days, so long as gustatory, cardiovascular and reticular-activating systems remained intact. Due to the small size of the hindbrain region, previous attempts using autologous blood injection could not

reproduce consistent hematomas, and consequently have received no further study (Chung and Haines, 1993; Cossu et al., 1994). These new models produced consistent bleeding inside the tissue borders of these small brain regions, with reproducible neurological and morphological features that can be intervened with neuroprotective treatments in future studies.

Summary

Concluding remarks

The hindbrain has many critical neural tracts and nuclei involved in processing and transmitting information between the cerebral cortexes and spine. Furthermore, injury to this area can be particularly devastating. This brain region may have less innate neurovascular protective mechanisms, and greater amount of cell death and injury in comparison to supratentorial strokes. A very limited, yet significant amount of experimental study has been done for ischemic posterior circulation stroke, while hemorrhage into the infratentorium has received no study to date. In spite of shared mechanisms between ischemic and hemorrhagic strokes, there is an urgent need to study ICH in the hindbrain. Future studies can use these new models of ICH, and an array of other ischemic models, to test interventions for reversing the mechanisms of injury in this brain region.

Acknowledgments

The content of this introductory chapter was partially supported by a grant from NIH NS53407 to John H. Zhang. The neuroimaging support was provided in part by a NASA cooperative agreement (NCCQ-XX) to Loma Linda University. The authors thank Jacqueline S. Coats and Pete Hayes with the animal imaging and figures.

CHAPTER TWO

CHARACTERIZATION OF THE BRAIN INJURY, NEUROBEHAVIORAL PROFILES AND HISTOPATHOLOGY IN A RAT MODEL OF CEREBELLAR HEMORRHAGE

Abstract

Spontaneous cerebellar hemorrhage (SCH) represents approximately 10% of all intracerebral hemorrhage (ICH), and is an important clinical problem of which little is known. This study stereotaxically infused collagenase (type VII) into the deep cerebellar paramedian white matter, which corresponds to the most common clinical injury region. Measures of hemostasis (brain water, hemoglobin assay, Evans blue, collagen-IV, ZO-1, and MMP-2 and MMP-9) and neurodeficit were quantified twenty-four hours later (Experiment 1). Long-term functional outcomes were measured over thirty days using the ataxia scale (modified Luciani), open field, wire suspension, beam balance and inclined plane (Experiment 2). Neurocognitive ability was assessed on the third week using the rotarod (motor learning), T-maze (working memory) and water-maze (spatial learning and memory) (Experiment 3), and this was followed by a histopathological analysis one week later (Experiment 4). Stereotaxic collagenase infusion caused dose-dependent elevations in brain edema,

neurodeficit, hematoma volume and blood-brain barrier rupture, while physiological variables remained stable. Most functional outcomes normalized by third week, while neurocognitive testing showed deficits parallel to the cystic-cavitary lesion at thirty days. All animals survived until sacrifice, and obstructive hydrocephalus did not develop. These results suggest that the model can generate important translational information about this subtype of ICH, and this could be used for future investigations of therapeutic mechanisms after cerebellar hemorrhage.

Introduction

Spontaneous (non-traumatic) cerebellar hemorrhage (SCH) results from the rupture of blood vessels within the cerebellum. SCH is a type of intracerebral hemorrhage (ICH) with an incidence of 1 in 33000 people every year, and accounts for 200,000 (10%) of around 2 million worldwide ICHs (Flaherty et al., 2005; Qureshi et al., 2009). Uncontrolled hematomal expansion causes abrupt ataxic neurological deterioration in nearly half of initially alert hospitalized patients (Rosenberg and Kaufman, 1976; St Louis et al., 1998) leading to a 40% mortality rate despite contemporary imaging and surgical methods (Flaherty et al., 2006; Hill and Silver, 2001). Almost 50% of these survivors will retain some cognitive deficits across motor-learning and visuospatial domains (Baillieux et al., 2008; Dolderer et al., 2004; Kelly et al., 2001; Strick et al., 2009).

The pathophysiological basis of SCH is poorly understood despite surgical approaches that presently diverge from all other forms of ICH (Jensen and St

Louis, 2005; Mendelow and Unterberg, 2007); and this underscores the need for translational research (NINDS, 2005). Our preliminary report demonstrated the feasibility of collagenase-induced *intra*cerebellar hemorrhage (Lekic et al., 2008). We had used a modification of an established (basal ganglia) ICH model (Rosenberg et al., 1990) that circumvented the hematomal dissections outside rodent cerebella which had complicated autologous blood injection approaches in this brain region previously (Cossu et al., 1991; Cossu et al., 1994).

While each experimental approach possesses drawbacks, the strength of collagenase-induced ICH resides with therapeutic investigations of hemostasis, neurobehavior, and histopathology (Andaluz et al., 2002; Foerch et al., 2008; Hartman et al., 2009; MacLellan et al., 2008; Rosenberg et al., 1990; Thiex et al., 2004). Therefore this study hypothesized that a rodent model of stereotaxic collagenase infusion could be used for translational purposes to extend the pathophysiological understanding of hematomal growth, brain edema, neurological deficit and brain atrophy after cerebellar hemorrhage (Baillieux et al., 2008; Dolderer et al., 2004; Kelly et al., 2001; Rosenberg and Kaufman, 1976; St Louis et al., 1998; Strick et al., 2009).

Materials and Methods

The Animals and Operative Procedure

96 adult male Sprague-Dawley rats (290–345g; Harlan, Indianapolis, IN) were used. All procedures were in compliance with the *Guide for the Care and Use of Laboratory Animals* and approved by the Animal Care and Use

Committee at Loma Linda University. Aseptic technique was used for all surgeries. Rats were anesthetized with isoflurane (4% induction, 2% maintenance, 70% N_2O and 30% O_2) and secured prone onto a stereotaxic frame (Kopf Instruments, Tujunga, CA) before making an incision over the scalp. The following stereotactic coordinates were then measured from bregma, to locate the deep cerebellar (paramedian) white matter tract: 11.6 mm (caudal), 2.4 mm (lateral), and 3.5 mm (deep). A borehole (1 mm) was drilled, and then a 27-gauge needle was inserted. Collagenase type VII (0.2 U/μL, Sigma, St Louis, MO) was infused by microinfusion pump (rate=0.2 μL/min, Harvard Apparatus, Holliston, MA). The syringe remained in place for 10 minutes to prevent back-leakage before being withdrawn. Then the borehole was sealed with bone wax, incision sutured closed, and animals allowed to recover. Control surgeries consisted of needle insertion alone. A thermostat-controlled heating blanket maintained the core temperature (37.0±0.5°C) throughout the operation. The animals were given free access to food and water upon recovery from anesthesia.

Experiment 1: Early Brain Injury at 24 Hours

Brain Water Content

Water content was measured using the wet-weight/ dry-weight method (Tang et al., 2004). Quickly after sacrifice the brains were removed and tissue weights were determined before and after drying for 24 hours in a 100°C oven, using an analytical microbalance (model AE 100; Mettler Instrument Co.,

Columbus, OH) capable of measuring with 1.0μg precision. The data was calculated as the percentage of water content: (wet weight - dry weight)/wet weight × 100.

Neuroscore

The composite neuroscore is a value of sensorimotor function consisting of the combined averages from wire suspension, beam balance and inclined plane (Colombel et al., 2002; Fernandez et al., 1998). The ataxic neuroscore is a modification of the Luciani scale, a summation of scores (maximum=9) measuring: body tone, limb-extension, and dyscoordination (Baillieux et al., 2008). Values are expressed as percent of sham; further details are provided (Experiment 2) below.

Animal Perfusion and Tissue Extraction

Animals were fatally anesthetized with isoflurane (≥%5) followed by cardiovascular perfusion with ice-cold PBS for the hemoglobin and Evans blue assays, and immunoblot analyses. The cerebella were then dissected and snap-frozen with liquid-nitrogen and stored in -80°C freezer, before spectrophotometric quantifications or protein extraction.

Hemorrhagic Volume

The spectrophotometric hemoglobin assay was performed as previously described (Tang et al., 2004), where extracted cerebellar tissue was placed in

glass test tubes with 3 mL of distilled water, then homogenized for 60 seconds (Tissue Miser Homogenizer; Fisher Scientific, Pittsburgh, PA). Ultrasonication for 1 minute lysed erythrocyte membranes, then centrifuged for 30 min, and Drabkin's reagent was added (Sigma-Aldrich) into aliquots of supernatant which reacted for 15 min. Absorbance, using a spectrophotometer (540 nm; Genesis 10uv; Thermo Fisher Scientific, Waltham, MA), was calculated into hemorrhagic volume on the basis of a standard curve (Choudhri et al., 1997).

Physiological Variables and Vascular Permeability

Under general anesthesia (operatively), the right femoral artery was catheterized for physiological variables, and re-assessed 24 hours later on the left side, followed by 2% intravenous Evans blue injection (5 mL/kg; 1 hr circulation). Extracted cerebellar tissue was weighed, homogenized in 1 mL PBS, then centrifuged for 30 minutes. After which 0.6 mL of the supernatant was added with equal volumes of trichloroacetic acid, followed by overnight incubation and re-centrifugation. The final supernatant underwent spectrophotometric quantification (615 nm; Genesis 10uv; Thermo Fisher Scientific, Waltham, MA) of extravasated dye, as described (Saria and Lundberg, 1983).

Western Blotting

As routinely done (Tang et al., 2004), the concentration of protein was determined using DC protein assay (Bio-Rad, Hercules, CA). Samples were subjected to SDS-PAGE, then transferred to nitrocellulose membrane for 80

minutes at 70 V (Bio-Rad). Blotting membranes were incubated for 2 hours with 5% nonfat milk in Tris-buffered saline containing 0.1% Tween 20 and then incubated overnight with the following primary antibodies: anti-collagen IV (1:500; Chemicon, Temecula, CA), anti-zonula occludens (ZO)-1 (1:500; Invitrogen Corporation, Carlsbad, CA), anti-matrix metalloproteinase (MMP)-2 and anti-matrix metalloproteinase (MMP)-9 (1:1500; Millipore, Billerica, MA). Followed by incubation with secondary antibodies (1:2000; Santa Cruz Biotechnology) and processed with ECL plus kit (Amersham Bioscience, Arlington Heights, Ill). Images were analyzed semiquantitatively using Image J (4.0, Media Cybernetics, Silver Spring, MD).

Experiment 2: Functional Outcome over Thirty Days

Animals were assessed with a battery of tests. The modified Luciani scale (3=severe, 2=moderate, 1=mild, 0=none) was a summation of scores (maximum=9) given for (a) decreased body tone, (b) ipsilateral limb-extensions, and (c) dyscoordination (Baillieux et al., 2008). For locomotion, the path length in open-topped plastic boxes (49cm-long, 35.5cm-wide, 44.5cm-tall) was digitally recorded for 30 minutes and analyzed by Noldus Ethovision tracking software (Hartman et al., 2009). For sensorimotor function, the falling latency was recorded (60 second cut-off) when all four limbs animals were placed perpendicularly onto a stationary horizontal beam balance (50cm-length, 5cm-diameter) or as the forelimbs grasped onto the wire suspension (40cm-length, 3mm-diameter) (Colombel et al., 2002). The inclined plane consisted of a box

(70cm-long, 20cm-wide, 10cm-tall) with an analog protractor and hinged base, elevated at 5 degree intervals until the animal slipped backwards (Fernandez et al., 1998).

Experiment 3: Neurocognitive Assessment at Third Week

Higher-order brain function was assessed using several different tests. For the rotarod task, a motor-learning paradigm was assessed by comparing pre-operative performance with four daily blocks on the third week after injury at days 21, 23, 25, and 27 (Hartman et al., 2009; Lekic et al., 2010). The apparatus consisted of a horizontal rotating cylinder (7cm-diameter x 9.5cm-wide, acceleration= 2 rpm/ 5 sec) requiring continuous walking to avoid falling, which was recorded by photobeam-circuit (Columbus Instruments). The T-Maze assessed short-term (working) memory (Hughes, 2004). Rats were placed into the stem (40 cm ×10 cm) of a maze and allowed to explore until one arm (46 cm × 10 cm) was chosen. From the sequence of ten trials, of left and right arm choices, the rate of spontaneous alternation (0% = none and 100% = complete, alternations/ trial) was calculated (Fathali et al., 2010; Zhou et al., 2009). For the Morris water-maze task, spatial learning and memory was assessed over four daily blocks on days 22, 24, 26 and 28 (Hartman et al., 2009; Lekic et al., 2010). The apparatus consisted of a metal pool (110cm diameter), filled to within 15cm of the upper edge, with a platform (11cm diameter) for the animal to escape onto that changed location for each block (maximum=60sec /trial), and digitally analyzed by Noldus Ethovision tracking software. Cued trials measured place

learning with the escape platform visible above water. Spatial trials measured spatial learning with the platform submerged and probe trials measured spatial memory once the platform was removed.

Experiment 4: Histopathological Analysis

Thirty days after collagenase infusion, the animals were fatally anesthetized with isoflurane (≥%5) followed by cardiovascular perfusion with ice-cold PBS and 10% paraformaldehyde. Brains were removed and postfixed in 10% paraformaldehyde then 30% sucrose (weight/volume) for 3 days. For all neuropathological analyses 10μm thick coronal sections were cut every 500 μm caudally on a cryostat (Leica Microsystems LM3050S), then mounted on poly-L-lysine-coated slides and stained. Morphometric analysis of cresyl violet slides involved computer-assisted (ImageJ 4.0, Media Cybernetics, Silver Spring, MD) hand delineation of the ventricles (lateral, third, cerebral aqueduct, and fourth), brainstem, cerebellum (ipsilateral and contralateral), cerebellar layers (white matter, molecular and granular) and lesioned area (cavity, cellular debris). Borderlines were based on criteria defined from stereologic studies using optical dissector principles (Andersen et al., 1992; Korbo et al., 1993; Oorschot, 1996). Brain volumes were calculated with established protocols: (Average [(Area of coronal section) - (lesion area)] × Interval × Number of sections) (Lekic et al., 2010; MacLellan et al., 2008). Purkinje cells were blindly counted in the viable (non-lesioned) brain tissues in accordance with standard technique (Schmidt et al., 2007; Song et al., 2007).

Statistical Analysis

Statistical significance was considered at $P<0.05$. Data was analyzed using analysis of variance (ANOVA), with repeated-measures (RM-ANOVA) for long-term neurobehavior. Significant interactions were explored with conservative Scheffe *post hoc* test, T-test (unpaired) and Mann-Whitney rank sum test when appropriate.

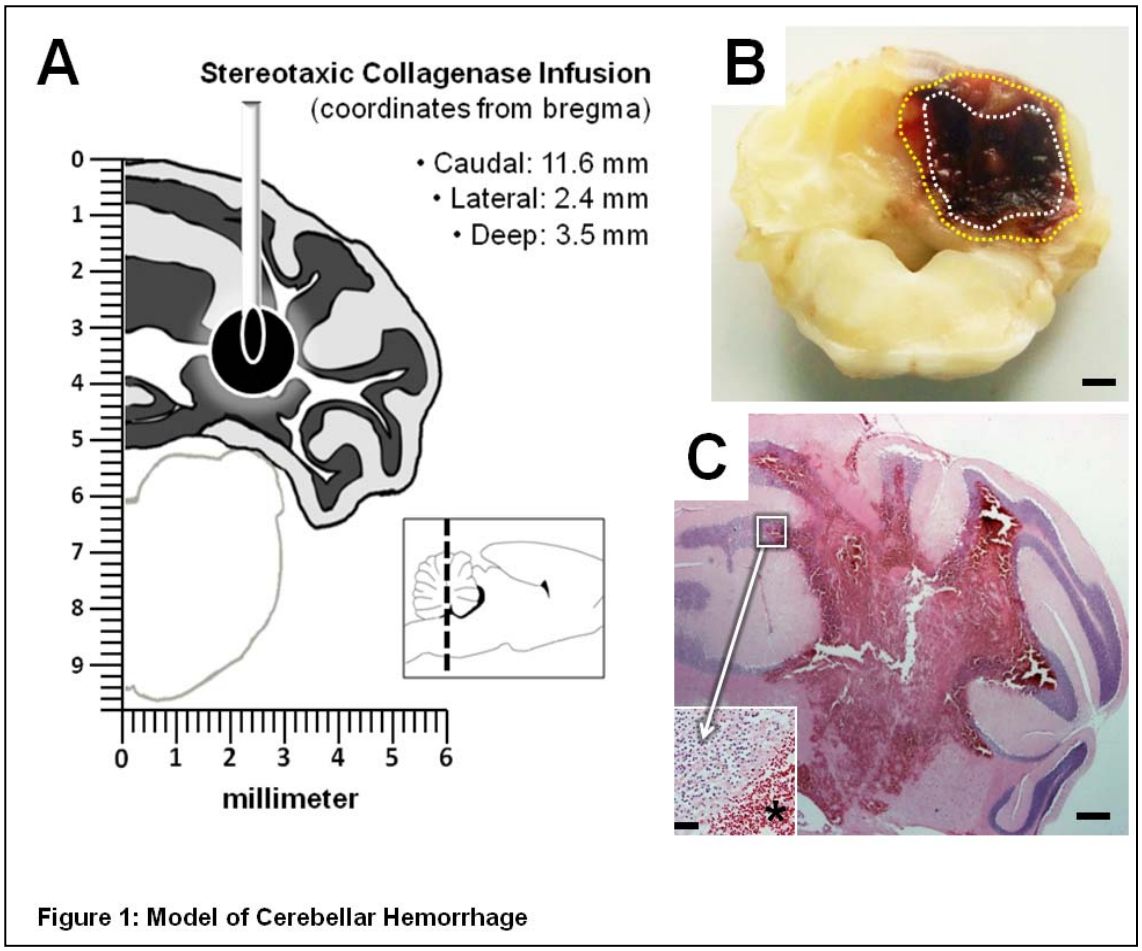

Figure 3. Experimental Model of Cerebellar Hemorrhage: (A) Schematic showing stereotaxic needle placement into the right paramedian white matter (inset demonstrating sagittal view with dotted-line at craniocaudal level). (B) Photograph of coronal section showing the hematoma surrounded by vasogenic edema at 24 hours after collagenase (0.6 units) infusion (outlined with dotted lines, bar= 1 mm) and (C) a representative H&E-stained cryosection illustrating hematomal location (bar= 0.5 mm) with inset showing hematomal (*) border (bar= 20 μm).

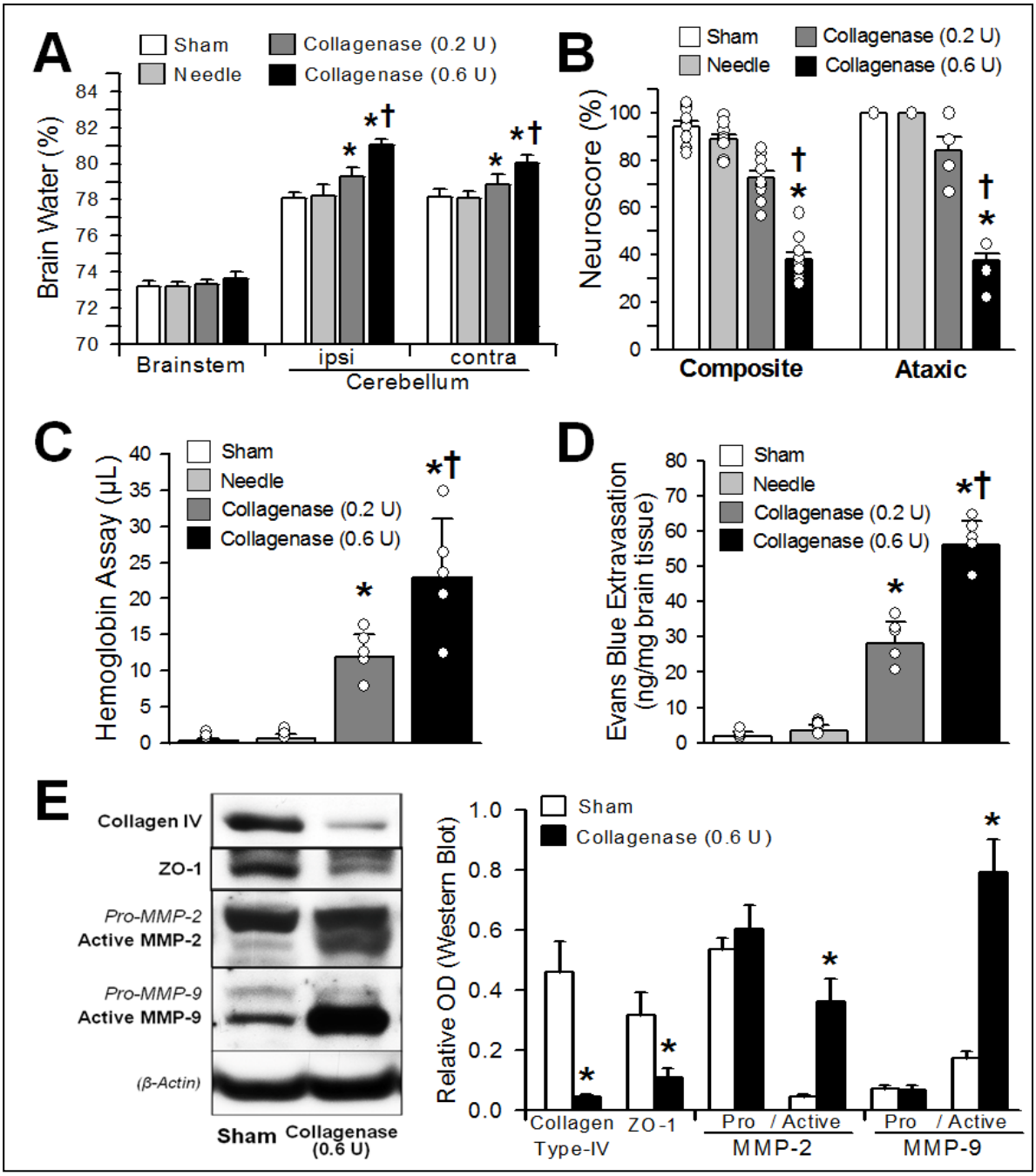

Figure 4. Early Brain Injury at 24 Hours: (A) Brain Water, (B) Neuroscore, (C) Hematomal Volume, (D) Vascular Permeability, and (E) Immunoblots (left) with semi-quantification (right) for Collagen-IV, ZO-1, MMP-2 and MMP-9. The values are expressed as mean ±SEM, n= 10 (neuroscore) and n= 5 (all others), *P<0.05 compared with controls (sham and needle trauma), †P<0.05 compared with collagenase infusion (0.2 units).

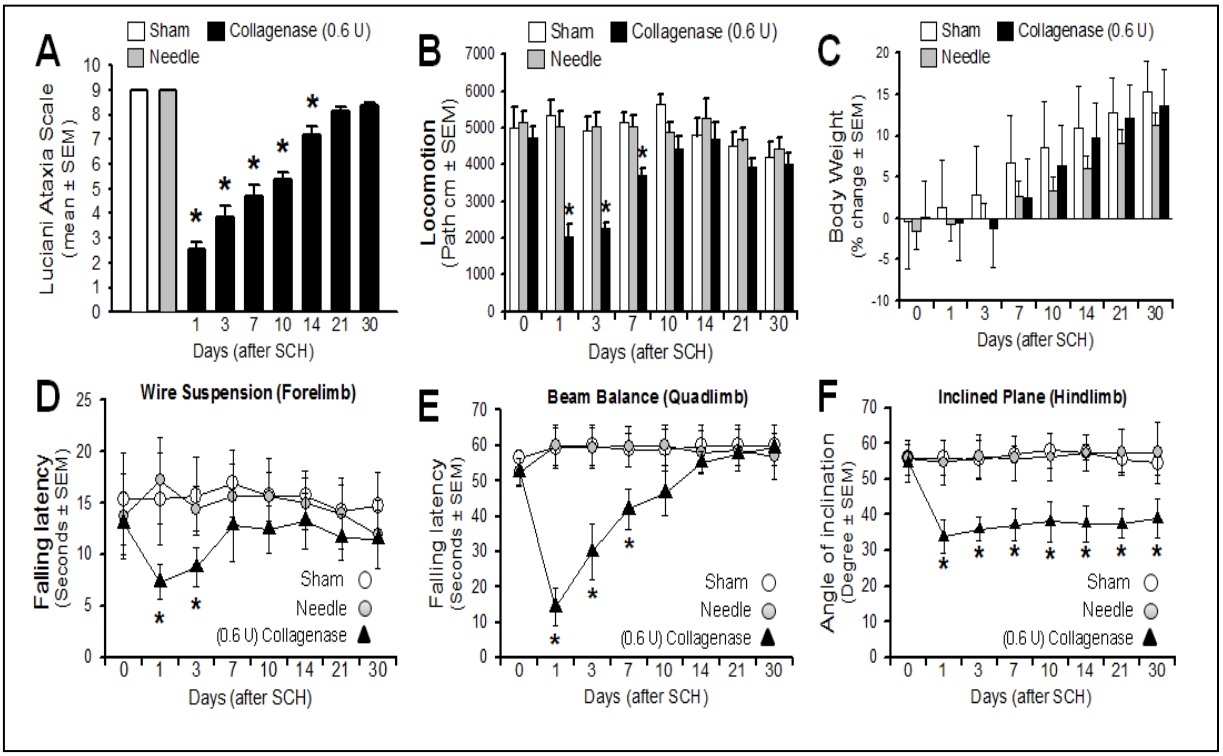

Figure 5. Functional Outcome over Thirty Days: (A) Luciani Ataxia Scale, (B) Locomotion, (C) Body Weight, (D) Wire Suspension, (E) Beam Balance, (F) Inclined Plane. The values are expressed as mean ±SEM, n=8 (per group), **P*<0.05 is comparing collagenase infusion (0.6 units, closed triangles) with controls (sham and needle trauma, open circles).

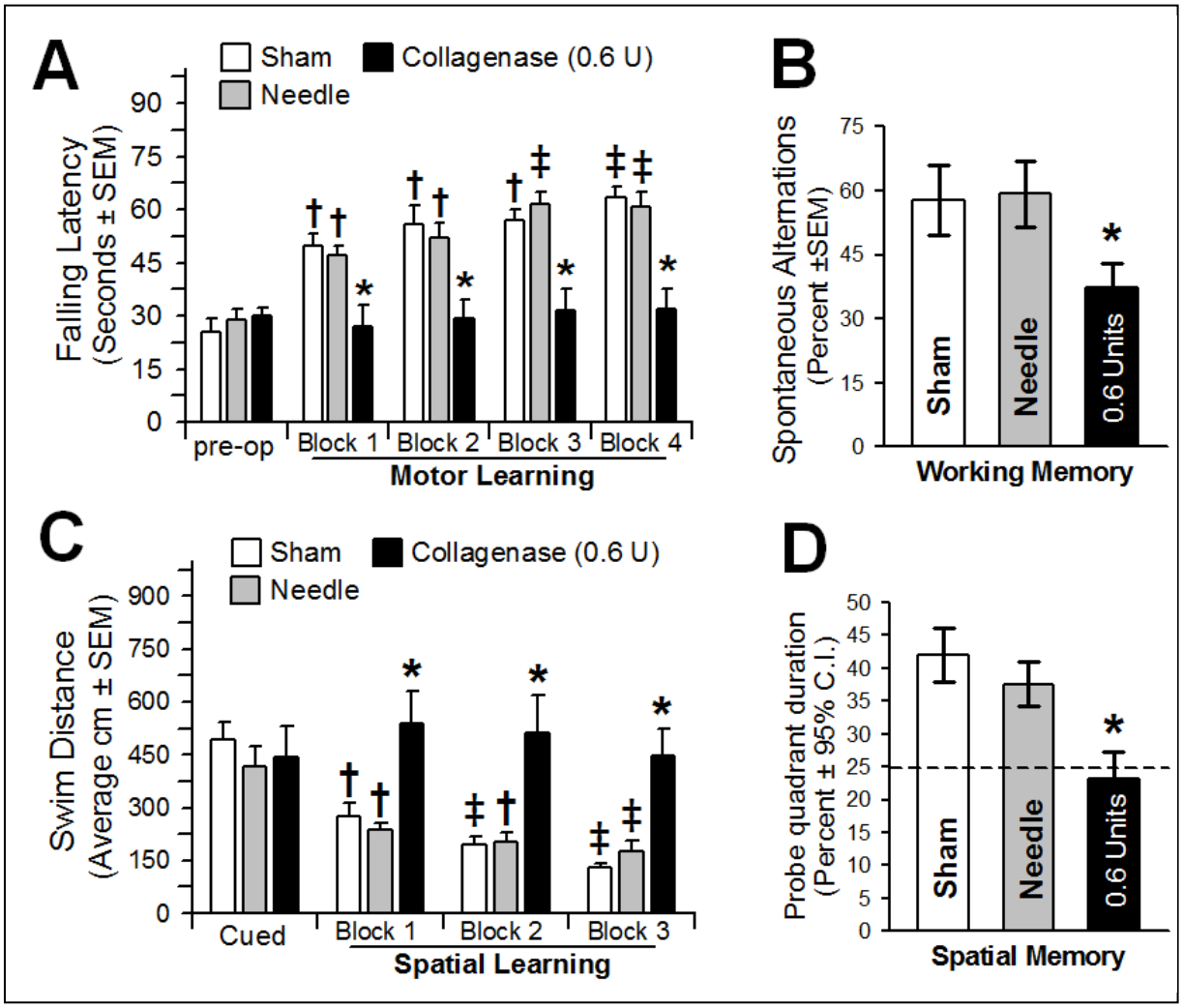

Figure 6. Neurocognitive Assessment at Third Week: (A) Motor learning was assessed by the change in the latency to fall off an accelerating rotarod (2 rpm/ 5 sec) pre-operatively and across four daily blocks. (B) Working memory was quantified by the number of spontaneous alternations in the T-Maze. (C) Spatial learning was assessed by the swim distance needed to find the visible (cued) versus the hidden (spatial) platforms in the water-maze. (D) Spatial memory was determined by the percent duration in the probe quadrant when the platform was removed. The values are expressed as mean ±SEM (rotarod, cued and spatial water-maze) and mean ±95th C.I. (probe quadrant), n=8 (per group), *P<0.05 compared with controls (sham and needle trauma), †P<0.05 compared with pre-operation (rotarod) or cued trials (spatial water-maze), and ‡ P<0.05 compared with Block 1 (rotarod and spatial water-maze)

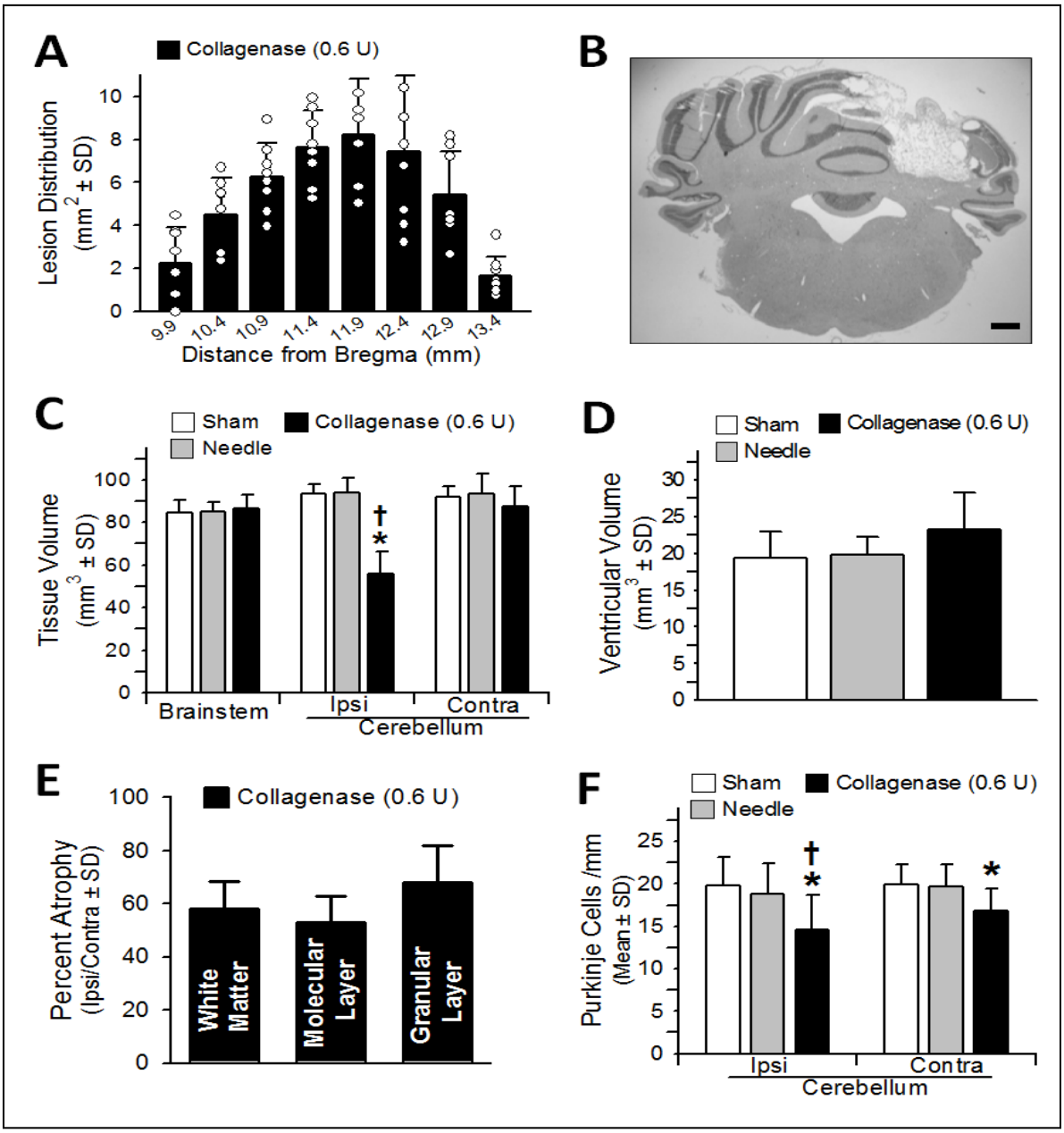

Figure 7. Histopathological Analysis: (A) Lesion distribution (mm^2) over the right cerebellar hemisphere. (B) Representative cryosection illustrating the cystic-cavitary lesion (scale bar= 1 mm). (C) Infratentorial brain tissue volume (mm^3). (D) Volume of the ventricles (mm^3). (E) Percent atrophy of white matter, molecular layer and granular layer, expressed as the volumetric difference between ipsilateral and contralateral folia. (F) Purkinje cell counts per millimeter (mm) over the intact (non-lesioned) areas of the cerebellum. Values expressed as mean ±SD, n=8 (per group), DCN indicates deep cerebellar nuclei, *P<0.05 compared with controls (sham and needle), †P<0.05 compared with contralateral side (tissue volume and purkinje cells).

Table 3. Arterial Blood Gas analysis (pH, PO_2, PCO_2), Mean Arterial Blood Pressure (BP), Heart Rate (HR), and Blood Glucose (BG) during and after (30 Min and 24 Hr) Collagenase Infusion (C.I.)

Group	pH	PO_2 (mm Hg)	PCO_2 (mm Hg)	BP (mm Hg)	HR (per min)	BG (mg/dL)
During C.I.						
Sham	7.33±0.03	184±35	45±3	82±6	338±40	209±62
Needle	7.36±0.03	184±21	42±4	90±7	357±16	245±69
C.I.—0.2 Units	7.33±0.10	187±17	43±7	93±7	366±42	212±42
C.I.—0.6 Units	7.34±0.09	192±43	45±12	93±9	372±28	217±50
30 Min after C.I.						
Sham	7.32±0.01	186±19	47±3	83±6	344±24	218±38
Needle	7.34±0.01	185±12	43±1	87±8	350±18	191±49
C.I.—0.2 Units	7.33±0.08	193±25	42±6	91±5	355±17	180±35
C.I.—0.6 Units	7.31±0.11	199±41	46±9	91±10	365±25	223±51
24 Hr after C.I.						
Sham	7.5±0.04	192±12	36±5	84±5	348±20	229±15
Needle	7.51±0.05	180±16	37±7	85±8	359±33	192±12
C.I.—0.2 Units	7.51±0.04	189±5	34±3	81±5	347±23	197±21
C.I.—0.6 Units	7.53±0.04	188±55	34±7	83±4	365±33	206±54

Values are mean ± SD. No significant differences among groups.

Results

Experimental Model of Cerebellar Hemorrhage

Systemic physiological variables were stable during and after the surgical procedure (see Table). Within 30 minutes after awaking from anesthesia, the collagenase infused animals exhibited ataxic gaits, ipsilateral limb extensions and decreased body tone. Pathological examinations at 24 hours revealed right cerebellar hemispheric hematomas surrounded with vasogenic edema, without subarachnoid or subdural bleeding and without ventricular obstruction, in spite of substantial amounts of bleeding (Fig. 1B and 1C). All animals survived though the end of the study and obstructive hydrocephalus did not develop.

Experiment 1: Early Brain Injury at 24 Hours

Unilateral collagenase infusion led to dose-dependent elevations of brain water, sensorimotor (composite neuroscore) deficit, hematoma volume, and vascular permeability ($P<0.05$, Fig. 2A-D). Immunoblots show significant activation of MMP-2 and -9, and degradation of collagen-IV and ZO-1 ($P<0.05$, Fig. 2E).

Experiment 2: Functional Outcome over Thirty Days

Infusion of collagenase (0.6 units) led to significant ataxic (modified Luciani), locomotor (open field) and sensorimotor (wire suspension, beam balance, inclined plane) deficits over the first week after injury ($P<0.05$, Fig. 3A-F). Body weight remained stable ($P>0.05$) and most functional parameters

recovered by three weeks after collagenase infusion, with the exception of inclined plane performance that showed only marginal change ($P<0.05$, Fig. 3F).

Experiment 3: Neurocognitive Assessment at Third Week

Collagenase infused (0.6 units) animals performed significantly worse than controls across all post-operative rotarod (motor) testing blocks ($P<0.05$, Fig. 4A) and were unable to improve upon their pre-operative performance ($P>0.05$), while, the controls improved their performance with each block ($P<0.05$). The T-Maze showed significant working memory differences ($P>0.05$, Fig. 4B), while for the water-maze, all groups performed the cued trials (place learning) equally ($P>0.05$, Fig. 4C). On the spatial blocks, however, collagenase infused animals performed significantly worse than controls ($P<0.05$), and were unable to improve upon the cued trials ($P>0.05$). As expected, the controls performed better with subsequent blocks ($P<0.05$) and with the overall spatial probe (memory trials; Fig. 4D).

Experiment 4: Histopathological Analysis

The topographic distribution of the lesion extended with a Gaussian distribution surrounding the level of injection at the paramedian white matter (11.6 mm caudal from bregma, Fig. 5A). The ipsilateral (right) cerebellum had an atrophic loss of brain tissue volume ($P<0.05$) without affecting the brainstem or contralateral side ($P>0.05$ Fig. 5B and 5C). All ventricles remained patent and were unchanged in size ($P>0.05$, Fig. 5D). The cystic cavitary lesion diminished

the cerebellar layers almost uniformly (P>0.05, Fig. 5E): white matter (60% ±10.6), molecular (53.1% ±9.8), and granular (67.8% ±14.2) without any significant atrophic differences between them. Purkinje cell density was decreased bilaterally, with the greatest diminishment on the ipsilateral (peri-lesion) side (P<0.05, Fig. 5F).

Discussion

An important translational research priority is the characterization of appropriate intracerebral hemorrhage (ICH) models (NINDS, 2005). Autologous blood or collagenase injection into the basal ganglia region of rodents represent the most common experimental approach for studying this condition (Andaluz et al., 2002; MacLellan et al., 2008; Xi et al., 2006). However, basal ganglia hemorrhage is a deep cerebral bleeding subtype, that as a group (basal ganglia, thalamus, and internal capsule), comprise no more than half of all cases (Flaherty et al., 2005), and animal models that represent the spectrum of ICH are highly needed (Gong et al., 2004; Song et al., 2007). Therefore this current study aimed to further establish a reproducible model of spontaneous cerebellar hemorrhage using stereotaxically injected collagenase (Lekic et al., 2008). This experimental paradigm could test therapeutic strategies for preventing the acutely devastating neurological deteriorations seen in patients (Jensen and St Louis, 2005; St Louis et al., 1998), and the application of cytoprotective interventions could further improve upon the lesion size and long-term

neurological deficit of the survivors (Dolderer et al., 2004; Kelly et al., 2001; Okauchi et al., 2009; Strick et al., 2009; Thach, 1996).

Clinically, uncontrolled hematomal expansion (vasogenic edema and re-bleeding) will necessitate surgery in nearly half of the hospitalized cerebellar hemorrhage patients (Rosenberg and Kaufman, 1976; St Louis et al., 1998); and this infratentorial location is an independent predictor of poor prognostic outcome (Hemphill et al., 2001). The (Class I) recommendation for a surgical approach after cerebellar hemorrhage differs from ICH in all other brain regions (Broderick et al., 2007) and highlights the unique pathophysiological aspects of this cerebellar disease (Mendelow et al., 2005). *In-vitro* studies further reveal divergence of injury mechanisms when comparing cerebellar with cortical neuronal cultures (Scorziello et al., 2001). In agreement, the wide-spread use of anticoagulants has been shown to disproportionately increase the rate of hemorrhage into the cerebellum compared with other brain regions (Flaherty et al., 2006). Our cerebellar hemorrhage model is therefore especially important, since collagenase infusion effectively evaluates hemostatic mechanisms with warfarin and tPA anticoagulation (Foerch et al., 2008; Thiex et al., 2004). Future experimental studies targeting hemostasis after cerebellar collagenase infusion in rats could translate into treatment strategies that improve the clinical course in conjunction with surgery (Broderick et al., 2007).

For intracerebral hemorrhage, the control of hemostasis is related both to the therapeutic approaches (Steiner and Bosel, 2010) and the propensity for injury through anticoagulant-use (Prabhakaran et al., 2010). The hemostatic

findings in this study were found to stand in agreement with experimental basal ganglia ICH in rats with regards to collagenase-induced brain edema, hematoma volume, blood-brain barrier rupture, and MMP-(2 and 9) activations (Power et al., 2003; Rosenberg and Navratil, 1997; Wang and Tsirka, 2005). On the other hand, this experimental model diverged from basal ganglia ICH, in failing to produce significant 24 hour sensorimotor and ataxia deficits with the typical collagenase dose of 0.2 units (MacLellan et al., 2008). This was circumvented for the long-term studies by choosing 0.6 units of collagenase to achieve a greater initial injury. This dose approximates that which was shown to avoid neurotoxicity in rodents (Matsushita et al., 2000), although cell death appears to be a less significant factor after cerebellar hemorrhage as compared to most other brain regions (Qureshi et al., 2003).

Collagenase infusion (0.6 units) yielded long-term neurobehavioral patterns that were very analogous with clinical reports after cerebellar hemorrhage in humans. Our study demonstrated that most neurological impairments resolved over the first three weeks of assessments, while motor-learning (rotarod) and cognitive ability (water-maze) remained impaired at one month after injury. In agreement, almost one-half of survivors from cerebellar hemorrhage will retain long-term deficits across motor-learning and visuospatial neurocognitive domains, even after full rehabilitation from ataxic losses of coordination, muscle tone, and overall strength (Baillieux et al., 2008; Dolderer et al., 2004; Kelly et al., 2001; Strick et al., 2009). On the other hand, our finding of marginal hind-limb recovery (inclined plane) was divergent from these clinical

manifestations. This is possibly a rodent-specific feature, due to the central placement of our cerebellar lesion that anatomically occupies the hind-limb control region; while the forelimb neurons are located more peripherally in the rodent cerebellum (Peeters et al., 1999). Future studies should apply therapeutic strategies, while extending the later neurobehavioral time-points, to better determine the reversibility of hind-limb function, cognitive ability and for translational application (Hua et al., 2006).

Neurobehavioral outcomes need to be correlated to a histopathological lesion, as a morphological measure of brain injury (Felberg et al., 2002; Hua et al., 2002). The cerebellum is organized into a geometric lattice with one-tenth the cerebral cortical volume, but four times the neuronal amount (Andersen et al., 1992). Thirty days after collagenase infusion, we found a well circumscribed cystic-cavitary lesion within the right cerebellum. The atrophy was focal and did not affect the contralateral side, similar to basal ganglia hemorrhage using rats (MacLellan et al., 2008). There also wasn't any difference between percent atrophy of the individual cerebellar layers; however, the early contralateral spreading of edema was followed by a bilateral loss in Purkinje cell density one month later. Since purkinje cells are the primary output of the cerebellum (Baillieux et al., 2008), this could be an additional contributor to the cognitive deficits in addition to the atrophic lesion alone. Taken together, these neuronal tissue losses represent a huge opportunity for neuroprotection strategies.

Cerebellar stroke is a human disease where clinical symptoms can be mapped to an acute lesion in a previously healthy cerebellum. In the past, these

clinical cases have allowed investigators to better understand the functional and morphological aspects of cerebellar recovery (Timmann et al., 2009). To date, rats undergoing hemicerebellectomy (HCb) had been the experimental correlates to this clinical cerebellar injury paradigm (Leggio et al., 2000). As an extension, our results indicate that collagenase infusion produces a lasting focal lesion and neurobehavioral profiles similar to cerebellar stroke patients. This approach overcomes several complications associated with rodent HCb, such as animal mortality and profound weight loss (Colombel et al., 2002). Therefore, future applications of collagenase infusion can have broad translational implications for cerebellar study.

Conclusion

We have characterized the early brain injury, neurobehavioral profiles, and histopathology in a highly reliable and easily reproducible experimental model of cerebellar hemorrhage in rats. Therapeutic strategies that mitigate the mass effect (brain edema and hematomal growth) and promote lasting neuroprotection (neurobehavioral and atrophic recovery) could lead to clinical approaches that afford these patients better outcomes in the future (Qureshi et al., 2009; Xi et al., 2006). These findings therefore provide a basis for characterizing the pathophysiological features of this disease, and establish a foundation for performing further preclinical therapeutic investigation.

Acknowledgements

This study was partially supported by a grant (NS053407) from the National Institutes of Health to J.H.Z. The authors report no conflicts of interest.

CHAPTER THREE

THE POSTPARTUM PERIOD OF PREGNANCY WORSENS BRAIN INJURY AND FUNCTIONAL OUTCOME AFTER CEREBELLAR HEMORRHAGE IN RATS

Abstract

Background: Intracerebral hemorrhage (ICH) is one of the most common causes of maternal deaths related to the postpartum period. This is a devastating form of stroke for which there is no available treatment. Although pre-menopausal females tend to have better outcomes after most forms of brain injury, the effects of pregnancy and child birth lead to wide maternal physiological changes that may predispose the mother to an increased risk for stroke and greater initial injury. Methods: Three different doses of collagenase were used to generate models of mild, moderate and severe cerebellar hemorrhage in postpartum female and male control rats. Brain water, blood-brain barrier rupture, hematoma size and neurological evaluations were performed 24 hours later. Results: Postpartum female rats had worsened brain water, blood-brain barrier rupture, hematoma size and neurological evaluations compared to their male counterparts. Conclusion: The postpartum state reverses the cytoprotective effects commonly associated with the hormonal neuroprotection of (pre-

menopausal) female gender, and leads to greater initial injury and worsened neurological function after cerebellar hemorrhage. This experimental model can be used for the study of future treatment strategies after postpartum brain hemorrhage, to gain a better understanding of the mechanistic basis for stroke in this important patient sub-population.

Introduction

Intracerebral hemorrhage (ICH) is a devastating complication of pregnancy that accounts for 1 out of 14 deaths within this sub-population in the United States (Bateman et al., 2006). ICH is the least treatable form of stroke (Ciccone et al., 2008) and has an approximate 20% mortality rate when related to pregnancy (Bateman et al., 2006). Survivors retain significant brain injury and life-long neurological deficits (Broderick et al., 1999; Skriver and Olsen, 1986), with most rehabilitating patients remaining unable to be “independent” six months later (Gebel and Broderick, 2000). Matched for age and gender, the relative risk for ICH is increased 30-fold during the postpartum period (Kittner et al., 1996).

Almost half the cases of postpartum ICH occur in patients with eclampsia (Sharshar et al., 1995), and this is associated with hemostatic elevations of aquaporin-4 (AQP4) expression, brain edema, and blood-brain barrier (BBB) disruption (Quick and Cipolla, 2005). The cerebellum contains some of the highest levels of AQP4 (Verkman, 2002), and is one of the brain locations with the greatest AQP4 increases during the postpartum period (Wiegman et al., 2008). Therefore this brain region could be a good model to study maternal mechanisms of ICH occurring during postpartum.

Clostridial collagenase is a stereotaxically infused enzyme that mimics spontaneous (ICH) vascular rupture, permiting investigations targeting hemostasis and neurobehavioral outcome (Andaluz et al., 2002; Foerch et al., 2008; Hartman et al., 2009; Lekic et al., 2010; MacLellan et al., 2008; Rosenberg et al., 1990; Thiex et al., 2004). We therefore hypothesized that unilateral cerebellar collagenase infusion in postpartum rats could model important clinical features (Baillieux et al., 2008; Dolderer et al., 2004; Kelly et al., 2001; Rosenberg and Kaufman, 1976; St Louis et al., 1998; Strick et al., 2009; Thach, 1996). This experimental approach may increase the pathophysiological understanding of this disease to direct future applications of therapeutic interventions (NINDS, 2005).

Materials and Methods

The Animals and General Procedures

109 adult Sprague-Dawley rats (290–345g; Harlan, Indianapolis, IN) were used. All procedures were in compliance with the *Guide for the Care and Use of Laboratory Animals* and approved by the Animal Care and Use Committee at Loma Linda University. Surgeries used isoflurane anesthesia with aseptic techniques and animals were given food and water during recovery (Hartman et al., 2009; Lekic et al., 2010).

Model of Cerebellar Hemorrhage

Anesthetized animals were secured prone onto a stereotaxic frame (Kopf Instruments, Tujunga, CA) before making an incision over the scalp. The

following stereotactic coordinates were measured from bregma: 11.6 mm (caudal), 2.4 mm (lateral), and 3.5 mm (deep). A (1 mm) borehole was drilled, and then a 27-gauge needle was inserted. Collagenase VII-S (0.2 U/μL, Sigma, St Louis, MO) was infused by microinfusion pump (rate=0.2 μL/min, Harvard Apparatus, Holliston, MA). The syringe remained in place for 10 minutes to prevent back-leakage before being withdrawn. Then the borehole was sealed with bone wax, incision sutured closed, and animals allowed to recover. Control surgeries consisted of needle insertion alone. A thermostat-controlled heating blanket maintained the core temperature (37.0±0.5°C) throughout the operation.

Cerebellar Water

Water content was measured using the wet-weight/ dry-weight method (Tang et al., 2004). Quickly after sacrifice the brains were removed and tissue weights were determined before and after drying for 24 hours in a 100°C oven, using an analytical microbalance (model AE 100; Mettler Instrument Co., Columbus, OH) capable of measuring with 1.0μg precision. The data was calculated as the percentage of water content: (wet weight - dry weight)/wet weight × 100.

Neurological Score

This was assessed using a modified Luciani scale (Baillieux et al., 2008) which is a summation of scores (maximum=9) given for (a) decreased body

tone, (b) ipsilateral limb-extensions, and (c) dyscoordination (0=severe, 1=moderate, 2=mild, 3=none). Scores are represented as percent of sham.

Animal Perfusion and Tissue Extraction

Animals were fatally anesthetized with isoflurane (≥%5) followed by cardiovascular perfusion with ice-cold PBS for the hemoglobin and Evans blue assays, and immunoblot analyses. The cerebella were then dissected and snap-frozen with liquid-nitrogen and stored in -80°C freezer, before spectrophotometric quantifications or protein extraction.

Hematoma Volume

The spectrophotometric hemoglobin assay was performed as previously described (Tang et al., 2004), where extracted cerebellar tissue was placed in glass test tubes with 3 mL of distilled water, then homogenized for 60 seconds (Tissue Miser Homogenizer; Fisher Scientific, Pittsburgh, PA). Ultrasonication for 1 minute lysed erythrocyte membranes (then centrifuged for 30 min) and Drabkin's reagent was added (Sigma-Aldrich) into aliquots of supernatant which reacted for 15 min. Absorbance, using a spectrophotometer (540 nm; Genesis 10uv; Thermo Fisher Scientific, Waltham, MA), was calculated into hemorrhagic volume on the basis of a standard curve (Choudhri et al., 1997).

Vascular Permeability

Under general anesthesia, the left femoral vein was catheterized for 2% intravenous Evans blue injection (5 mL/kg; 1 hr circulation). Extracted cerebellar tissue was weighed, homogenized in 1 mL PBS, then centrifuged for 30 minutes. After which 0.6 mL of the supernatant was added with equal volumes of trichloroacetic acid, followed by overnight incubation and re-centrifugation. The final supernatant underwent spectrophotometric quantification (615 nm; Genesis 10uv; Thermo Fisher Scientific, Waltham, MA) of extravasated dye, as described (Saria and Lundberg, 1983).

Western Blotting

As routinely done (Tang et al., 2004), the concentration of protein was determined using DC protein assay (Bio-Rad, Hercules, CA). Samples were subjected to SDS-PAGE, then transferred to nitrocellulose membrane for 80 minutes at 70 V (Bio-Rad). Blotting membranes were incubated for 2 hours with 5% nonfat milk in Tris-buffered saline containing 0.1% Tween 20 and then incubated overnight with the following primary antibodies: anti- AQP4 (1:200; Santa Cruz Biotechnology, Santa Cruz, CA), anti-collagen IV (1:500; Chemicon, Temecula, CA), anti-zonula occludens (ZO)-1 (1:500; Invitrogen Corporation, Carlsbad, CA). Followed by incubation with secondary antibodies (1:2000; Santa Cruz Biotechnology) and processed with ECL plus kit (Amersham Bioscience, Arlington Heights, Ill). Images were analyzed semiquantitatively using Image J (4.0, Media Cybernetics, Silver Spring, MD).

Statistical Analysis

Statistical significance was considered at $P<0.05$. Data was analyzed using analysis of variance (ANOVA). Significant interactions were explored with T-test (unpaired) and Mann-Whitney rank sum test when appropriate.

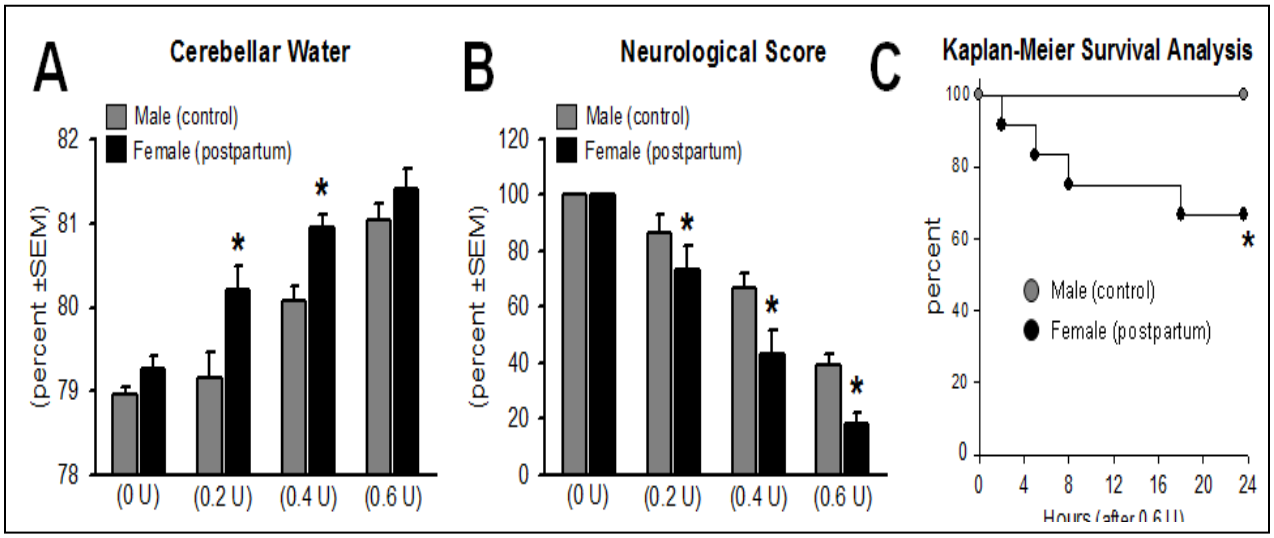

Figure 8. Postpartum Worsens Outcomes at 24 h after Collagenase Infusion.
(A) Cerebellar Water, (B) Neurological Score, and (C) Survival Analysis, groups consisted of male (control) and female (postpartum), receiving doses of 0, 0.2, 0.4 and 0.6 units collagenase. The values are expressed as mean ±SEM, n= 5 (per group), *P<0.05 compared with male (control)

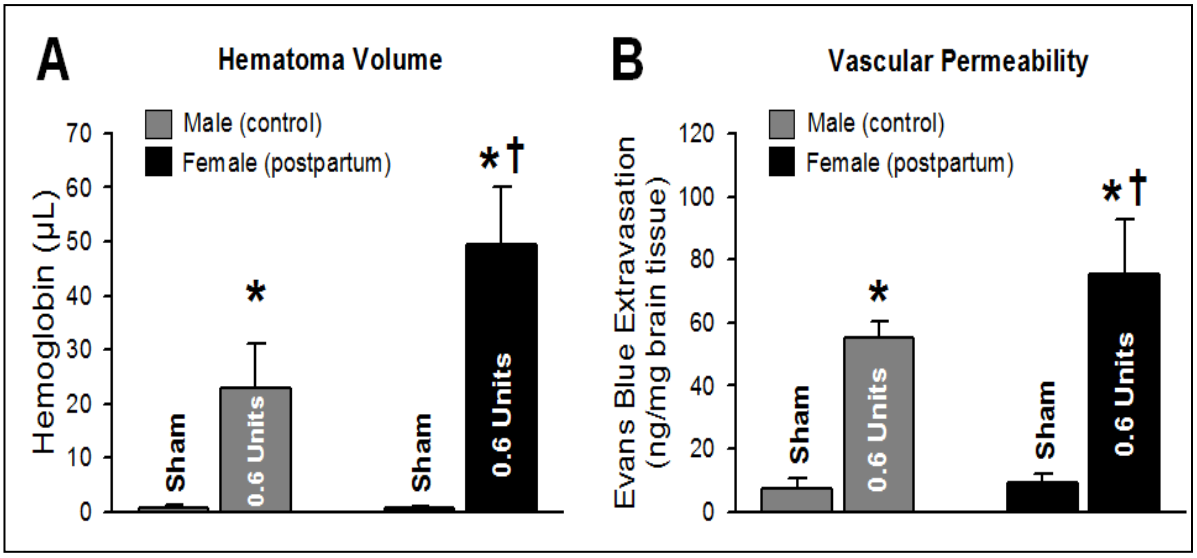

Figure 9. Postpartum Increases Vascular Rupture at 24 h after Collagenase Infusion. (A) Hematoma Volume, and (B) Vascular Permeability, the values are expressed as mean ±SD, groups consisted of male (control) and female (postpartum), receiving doses of 0 and 0.6 units collagenase, n= 5 (per group), *P<0.05 compared with respective shams, and †P<0.05 compared with male (0.6 units, control)

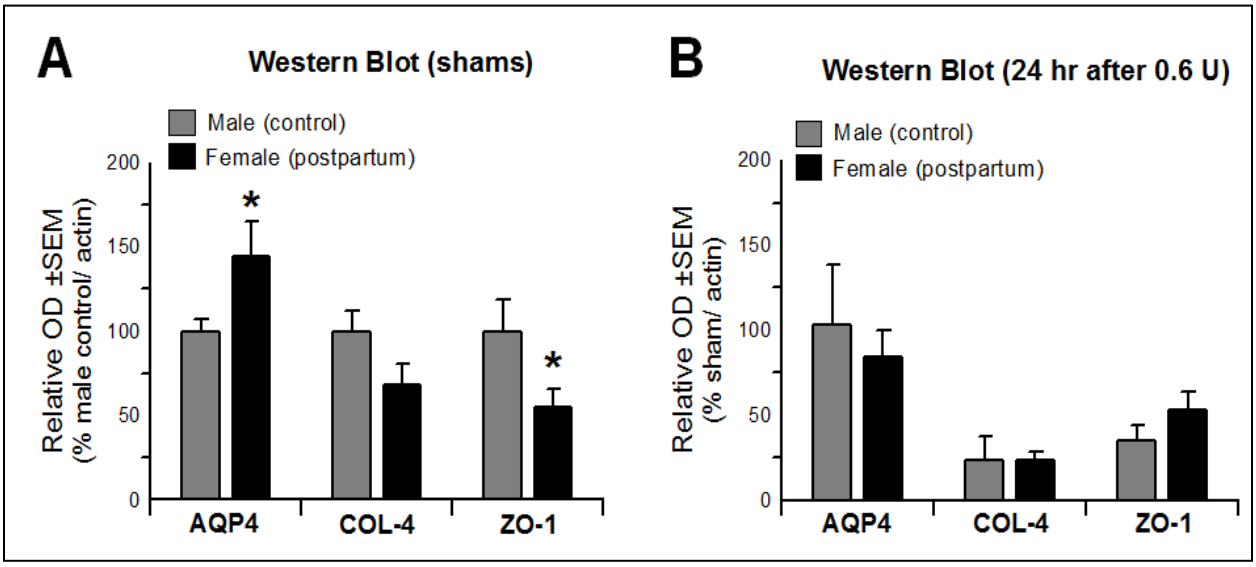

Figure 10. Postpartum Rats Have Increased Vascular Vulnerability. (A and B) Semi-quantification of immunoblots for AQP4, collagen-IV (COL-4), and ZO-1, groups consisted of male (control) and female (postpartum), receiving doses of 0 and 0.6 units collagenase. The values are expressed as mean ±SEM, n= 5 (per group), *P<0.05 compared with male (control)

Results

Collagenase infusion led to dose-dependent elevations of cerebellar water and neurodeficit (Figures 8A and 8B). Compared to male controls, cerebellar water was significantly elevated in postpartum females at 0.2 and 0.4 units collagenase, and neurodeficit across all doses ($P<0.05$). Kaplan-Meier survival analysis demonstrated a significantly increased mortality rate (Figure 8C, $P<0.05$) in postpartum females (approx. 30%) compared to male controls (0%). Collagenase infusion (0.6 U) led to a greater hematoma size (Figure 9A) and vascular permeability (Figure 9B) in postpartum females, compared to male controls ($P<0.05$). Immunoblots of shams (Figure 10A) are showing greater AQP4, and diminished COL-4 (collagen-IV) and ZO-1, expressions in postpartum females compared to male controls ($P<0.05$), while collagenase infusion (0.6 U) injury was equivalent, and did not cause any additional changes compared to respective shams (Figure 10B, $P<0.05$).

Discussion

Intracerebral hemorrhage (ICH) is the least treatable form of stroke clinically, and is a devastating complication after pregnancy accompanied by life-long neurodeficits (Bateman et al., 2006; Broderick et al., 1999; Ciccone et al., 2008; Gebel and Broderick, 2000; Kittner et al., 1996; Skriver and Olsen, 1986). This study infused collagenase into the unilateral (right) side of the cerebellar hemisphere of postpartum rats, as an approach to model these features, since

available animal models to study the pathophysiological basis of these outcomes is lacking.

Our results are in support of the clinical evidence for cerebral vascular vulnerability in the postpartum period. Around half the cases of ICH in this patient population will have the eclampsia (Sharshar et al., 1995), and this is related to hemostatically relevant increases of aquaporin-4 (AQP4) expression, blood-brain barrier (BBB) disruption, and brain edema (Quick and Cipolla, 2005). In agreement, we found greater AQP4, and diminished COL-4 (collagen-IV) and ZO-1, expressions in the cerebella of postpartum female shams compared to the male controls. The collagenase model is an ideal method for study, since it did not alter these levels any further, however, the increased vascular vulnerability in postpartum animals, led to greater brain edema, neurodeficit, BBB-rupture and hematoma size across most doses studied. The lack of significant difference in cerebellar water at the highest collagenase dose (0.6 U) is likely either a reflection of mortality (i.e. severely injured animals died), or due to the high baseline AQP4 expressions leading to an edematous outflow.

In summary, we have characterized a highly reliable and easily reproducible experimental model of intracerebral hemorrhage using postpartum rats. Since the cerebellum contains some of the highest levels of AQP4 (Verkman, 2002) with the greatest AQP4 increase during the postpartum period (Wiegman et al., 2008), this ICH model provides a basis for studying the clinical and pathophysiological features of this disease, while establishing a foundation for performing further preclinical therapeutic investigations.

Acknowledgements

This study was partially supported by a grant (NS053407) from the National Institutes of Health to J.H.Z. The authors report no conflicts of interest.

CHAPTER FOUR

EVALUATION OF HEMOSTASIS, NEUROCOGNITION, AND NEUROPATHOLOGICAL CONSEQUENCES USING A MODEL OF PONTINE HEMORRHAGE IN RATS

Abstract

Background and Purpose: Pontine hemorrhage (PH) is the most devastating type of stroke and yet there is no available treatment. The goal of this present study was to develop an instructive model to gain a better pathophysiological understanding, while further testing of therapeutic strategies. Methods: Intraparenchymal bleeding at the brainstem was achieved by stereotaxic infusion of collagenase type VII. Measures of hemostasis (brain water, hemoglobin assay, Evans blue, collagen-IV, ZO-1, and MMP-2 and MMP-9) and sensorimotor function were quantified twenty-four hours later. Thirty day functional outcome was evaluated by modified Garcia scale, open field, wire suspension, beam balance and inclined plane. Neurocognitive ability was assessed by the rotarod and water-maze on the third week. This was followed by a histopathological analysis one week later. Results: Collagenase infusion led to dose-dependent increases in brain edema, neurodeficit, hematoma volume and blood-brain barrier rupture, while physiological variables remained stable.

Functional outcome was nearly recovered at three weeks. Neurocognitive testing showed motor and spatial learning deficits, as related to the cystic-cavitary lesion at thirty days. Conclusions: This study characterized several hemostatic, neurocognitive, and neuropathological features to model the clinical consequence of pontine hemorrhage in humans. Testing of therapeutic strategies could improve upon these parameters, while expanding the clinical knowledge about this disease.

Introduction

Non-traumatic (spontaneous) pontine hemorrhage results from the rupture of blood vessels within the brainstem. There is an annual incidence of 1 per 50 000 population (Flaherty et al., 2005), and will account for 140 000 (7%) (Flaherty et al., 2005) of about 2 million worldwide intracerebral hemorrhages (ICHs) each year (Qureshi et al., 2009). Pontine hemorrhage can also complicate traumatic brain-injury (TBI) (Zuccarello et al., 1983) and up to 20% of malignant middle cerebral artery (MCA) infarctions (Jaramillo et al., 2006). It is the most devastating type of ICH, with the worst prognosis, having an approximate 65% mortality rate (Flaherty et al., 2006; Zia et al., 2009).

Pontine hemorrhage (PH) is a poorly understood disease without an instructive model for experimental purposes (Lekic and Zhang, 2008). Hematomal growth is highly associated with worsened patient outcomes (Balci et al., 2005; Broderick et al., 1993; Dziewas et al., 2003; Goto et al., 1980; Wijdicks and St Louis, 1997). Up to half the survivors will have disabling sensorimotor

and cognitive neurological deficits (Maeshima et al., 2010; Masiyama et al., 1985; Nys et al., 2007), with less disability after small unilateral pontine hematomas (Burns et al., 1980; Chung and Park, 1992; Kushner and Bressman, 1985; Payne et al., 1978). An upmost research priority is the development and validation of appropriate ICH animal models for translating human conditions (NINDS, 2005). Prolonged infusions into the rat pontine tegmentum (nucleus oralis) are tolerated without neurological injury (Occhiogrosso et al., 2003), and stereotaxic collagenase infusion is one the most commonly used methods in experimental ICH studies (MacLellan et al., 2008; Rosenberg et al., 1990). This enzyme lyses the extracellular-matrix around blood vessels to mimic spontaneous vascular rupture as an approach enabling investigations of cerebrovascular hemostasis, neurological outcomes and neuropathology (Andaluz et al., 2002; Foerch et al., 2008; Hartman et al., 2009; Lekic et al., 2010; MacLellan et al., 2008; Rosenberg et al., 1990; Thiex et al., 2004).

In this study, we hypothesized that unilateral pontine collagenase infusion in rats, would model features similar to pontine hemorrhage in humans (Balci et al., 2005; Broderick et al., 1993; Burns et al., 1980; Chung and Park, 1992; Dziewas et al., 2003; Goto et al., 1980; Kushner and Bressman, 1985; Maeshima et al., 2010; Masiyama et al., 1985; Nys et al., 2007; Payne et al., 1978; Wijdicks and St Louis, 1997). Using this model, the application of therapeutic strategies can be tested to improve outcome parameters and the pathophysiological understanding of this disease (NINDS, 2005).

Materials and Methods

The Animals and General Procedures

Adult male Sprague-Dawley rats (290–345g; Harlan, Indianapolis, IN) were used for this study. All procedures were in compliance with the *Guide for the Care and Use of Laboratory Animals* and approved by the Animal Care and Use Committee at Loma Linda University. Surgeries used isoflurane anesthesia (4% induction, 2% maintenance, 70% N_2O and 30% O_2) with aseptic technique and animals were given food and water during recovery (Hartman et al., 2009; Lekic et al., 2010).

Experimental Model of Pontine Hemorrhage

Anesthetized animals were secured prone onto a stereotaxic frame (Kopf Instruments, Tujunga, CA) before making an incision over the scalp. The following stereotactic coordinates were measured from bregma: 8.5 mm (caudal), 1.4 mm (lateral), and 7 mm (deep). A (1 mm) borehole was drilled, and then a 27-gauge needle was inserted. Collagenase VII-S (0.2 U/μL, Sigma, St Louis, MO) was infused by microinfusion pump (rate= 0.2 μL/min, Harvard Apparatus, Holliston, MA). The syringe remained in place for 10 minutes to prevent back-leakage before being withdrawn. Then the borehole was sealed with bone wax, incision sutured closed, and animals allowed to recover. Control surgeries consisted of needle insertion alone. A thermostat-controlled heating blanket maintained the core temperature (37.0±0.5°C) throughout the operation.

Brain Water Content

Water content was measured using the wet-weight/ dry-weight method (Tang et al., 2004). Quickly after sacrifice the brains were removed and tissue weights were determined before and after drying for 24 hours in a 100°C oven, using an analytical microbalance (model AE 100; Mettler Instrument Co., Columbus, OH) capable of measuring with 1.0μg precision. The data was calculated as the percentage of water content: (wet weight - dry weight)/wet weight × 100.

Composite (sensorimotor) Neuroscore

This is a value of sensorimotor function consisting of combined averages from wire suspension, beam balance and inclined plane (expressed as percent of sham), and further details are provided (below) (Colombel et al., 2002; Fernandez et al., 1998).

Animal Perfusion and Tissue Extraction

Animals were fatally anesthetized with isoflurane (≥%5) followed by cardiovascular perfusion with ice-cold PBS for the hemoglobin and Evans blue assays, and immunoblot analyses. The brainstems were then dissected and snap-frozen with liquid-nitrogen and stored in -80°C freezer, before spectrophotometric quantifications or protein extraction.

Hemorrhagic Volume

The spectrophotometric hemoglobin assay was performed as previously described (Tang et al., 2004), where extracted brainstem tissue was placed in glass test tubes with distilled water (total volume 3 mL) then homogenized for 60 seconds (Tissue Miser Homogenizer; Fisher Scientific, Pittsburgh, PA), ultrasound on ice for 1 minute to lyse erythrocyte membranes, centrifugation for 30 min at 4°C and then added Drabkin's reagent (400 µL; Sigma-Aldrich) into 100 µL aliquots of the supernatant that were allowed to react for 15 min. Absorbance was read using a spectrophotometer (540 nm; Genesis 10uv; Thermo Fisher Scientific, Waltham, MA) and the hemorrhagic volume for each brainstem was calculated on the basis of a standard curve (Choudhri et al., 1997).

Physiological Variables and Vascular Permeability

Under general anesthesia (operatively), the right femoral artery was catheterized for physiological variables, and re-assessed 24 hours later on the left side, followed by 2% intravenous Evans blue injection (5 mL/kg; 1 hr circulation). As done routinely (Shimamura et al., 2006), the extracted brainstem tissue was weighed, homogenized in 1 mL of phosphate-buffered saline, and then centrifuged for 30 minutes to which 0.6 mL of the supernatant was added to an equal volume of trichloroacetic acid, followed by overnight incubation at 4°C and re-centrifugation. The final supernatant underwent spectrophotometric

quantification (615 nm; Genesis 10uv; Thermo Fisher Scientific, Waltham, MA) of extravasated dye (Saria and Lundberg, 1983).

Western Blotting

As routinely done (Tang et al., 2004), the concentration of protein was determined using DC protein assay (Bio-Rad, Hercules, CA). Samples were subjected to SDS-PAGE, then transferred to nitrocellulose membrane for 80 minutes at 70 V (Bio-Rad). Blotting membranes were incubated for 2 hours with 5% nonfat milk in Tris-buffered saline containing 0.1% Tween 20 and then incubated overnight with the following primary antibodies: anti-collagen IV (1:500; Chemicon, Temecula, CA), anti-zonula occludens (ZO)-1 (1:500; Invitrogen Corporation, Carlsbad, CA), anti-matrix metalloproteinase (MMP)-2 and anti-matrix metalloproteinase (MMP)-9 (1:1500; Millipore, Billerica, MA). Followed by incubation with secondary antibodies (1:2000; Santa Cruz Biotechnology) and processed with ECL plus kit (Amersham Bioscience, Arlington Heights, Ill). Images were analyzed semiquantitatively using Image J (4.0, Media Cybernetics, Silver Spring, MD).

Functional Outcome over 30 Days

Animals were assessed with a battery of tests. The modified Garcia scale was a summation of scores (maximum= 40) for neurological assessment, as routinely done (Hartman et al., 2009). For locomotion, the path length in open-topped plastic boxes (49cm-long, 35.5cm-wide, 44.5cm-tall) was digitally

recorded for 30 minutes and analyzed by Noldus Ethovision tracking software (Hartman et al., 2009). The falling latency was recorded (60 second cut-off) when all four limbs animals were placed perpendicularly onto a stationary horizontal beam balance (50cm-length, 5cm-diameter) and as the forelimbs grasped onto the wire suspension (40cm-length, 3mm-diameter) (Colombel et al., 2002). The inclined plane consisted of a box (70cm-long, 20cm-wide, 10cm-tall) with an analog protractor and hinged base, elevated at 5 degree intervals until the animal slipped backwards (Fernandez et al., 1998), and body weights were measured as described (Hartman et al., 2009).

Motor and Spatial Learning Assessment at 3 Weeks

For the rotarod task, motor-learning was assessed pre-operatively and on four daily blocks at the third week after injury (days 21, 23, 25, and 27) (Hartman et al., 2009; Lekic et al., 2010). The apparatus consisted of a horizontal rotating cylinder (7cm-diameter x 9.5cm-wide, acceleration= 2 rpm/ 5 sec) requiring continuous walking to avoid falling, which was recorded by photobeam-circuit (Columbus Instruments). For the Morris water-maze task, spatial learning and memory was assessed on four daily blocks (days 22, 24, 26 and 28) (Hartman et al., 2009; Lekic et al., 2010). The apparatus consisted of a metal pool (110cm diameter), filled to within 15cm of the upper edge, with a platform (11cm diameter) for the animal to escape onto that changed location for each block (maximum=60sec /trial), and digitally analyzed by Noldus Ethovision tracking software. Cued trials measured place learning with the escape platform visible

above water. Spatial trials measured spatial learning with the platform submerged and probe trials measured spatial memory once the platform was removed.

Statistical Analysis

Statistical significance was considered at $P<0.05$. Data was analyzed using analysis of variance (ANOVA), with repeated-measures (RM-ANOVA) for long-term neurobehavior. Significant interactions were explored with conservative Scheffe *post hoc* test, T-test (unpaired) and Mann-Whitney rank sum test when appropriate.

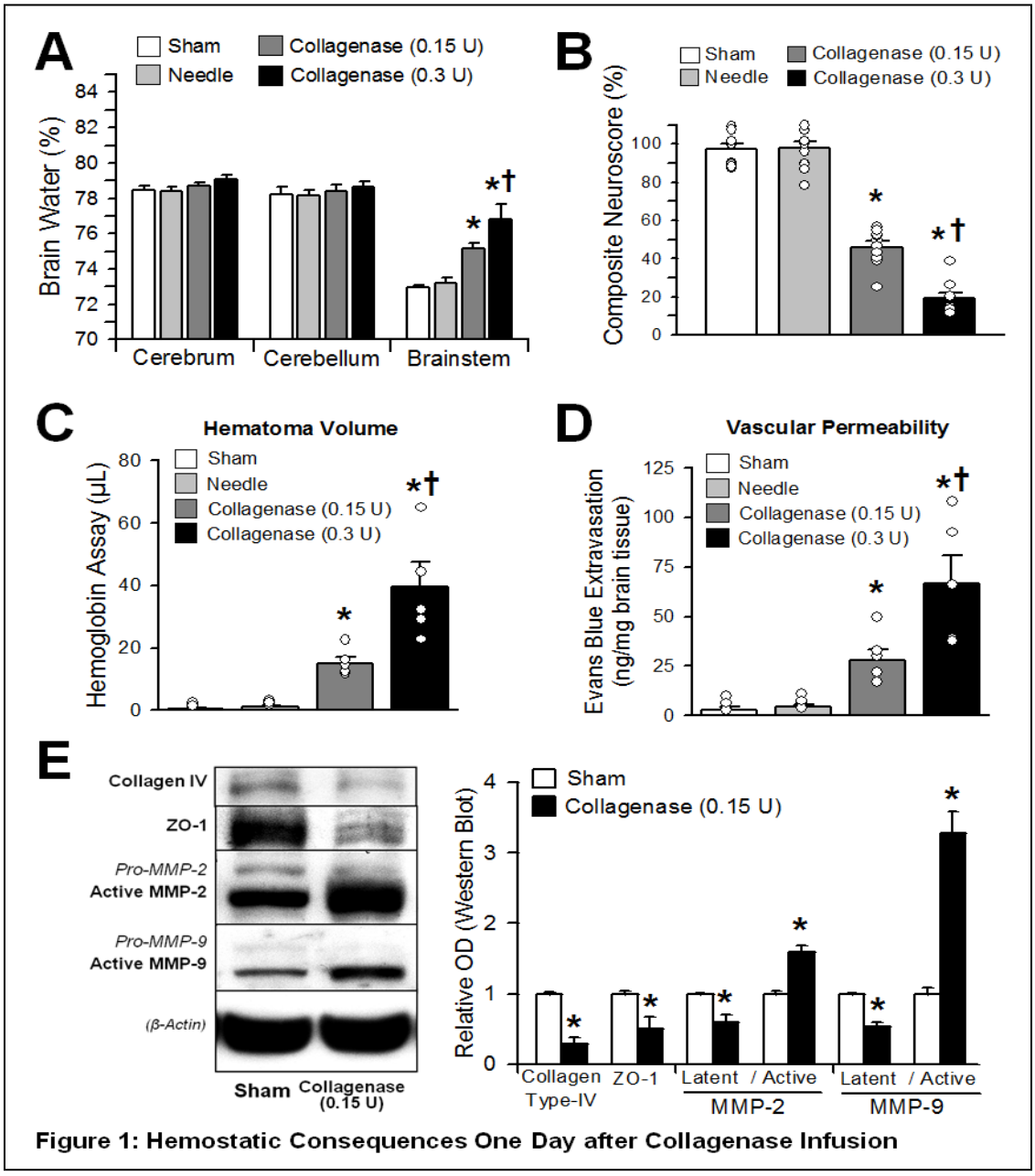

Figure 11. (A) Brain Water, (B) Composite Neuroscore, (C) Hematoma Volume, (D) Vascular Permeability, and (E) Immunoblots (left) with semi-quantification (right) for Collagen-IV, ZO-1, MMP-2 and MMP-9. Values expressed as mean ±SEM, n= 10 (composite neuroscore) and n= 5 (all others), *P<0.05 compared with controls (sham and needle), †P<0.05 compared with collagenase infusion (0.15 units)

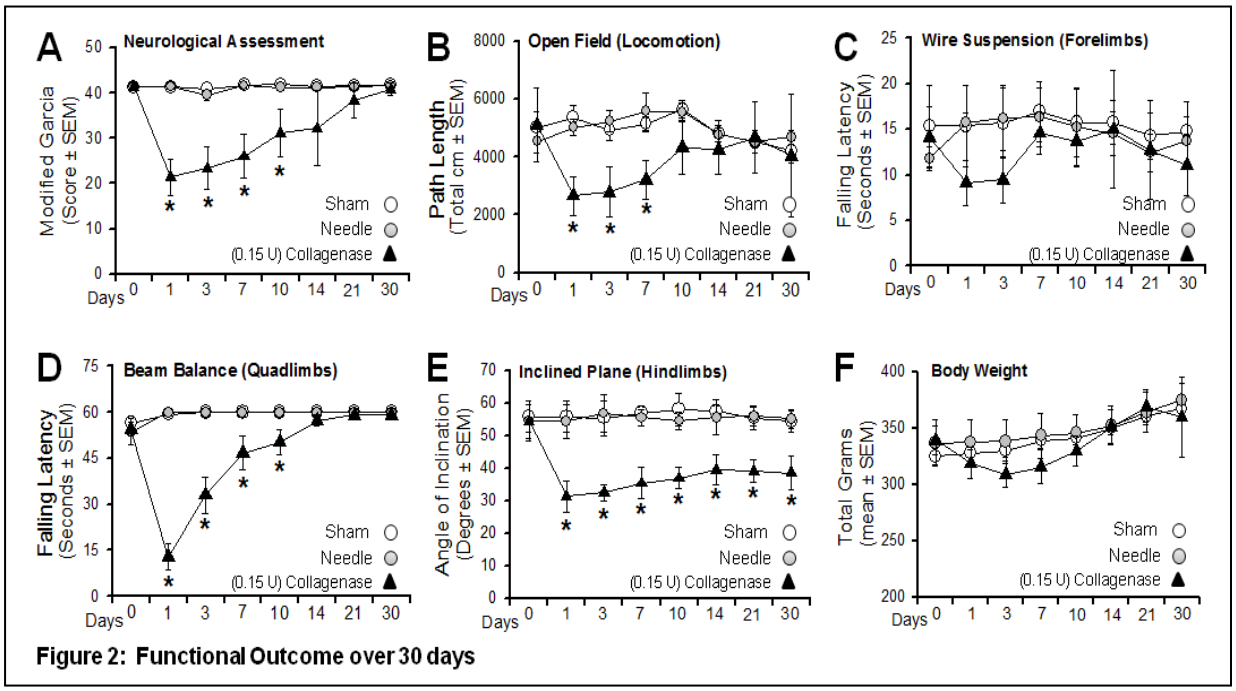

Figure 2: Functional Outcome over 30 days

Figure 12. (A) Neurological (modified Garcia scale), (B) Locomotion (open field), and (C-E) Sensorimotor (wire suspension for forelimbs, beam balance for quad-limb, inclined plane for hind-limbs) Assessments. (F) Body Weight. Values expressed as mean ±SEM, n=8 (per group), *P<0.05 is comparing collagenase infusion (0.15 units, closed triangles) with controls (sham and needle, open circles)

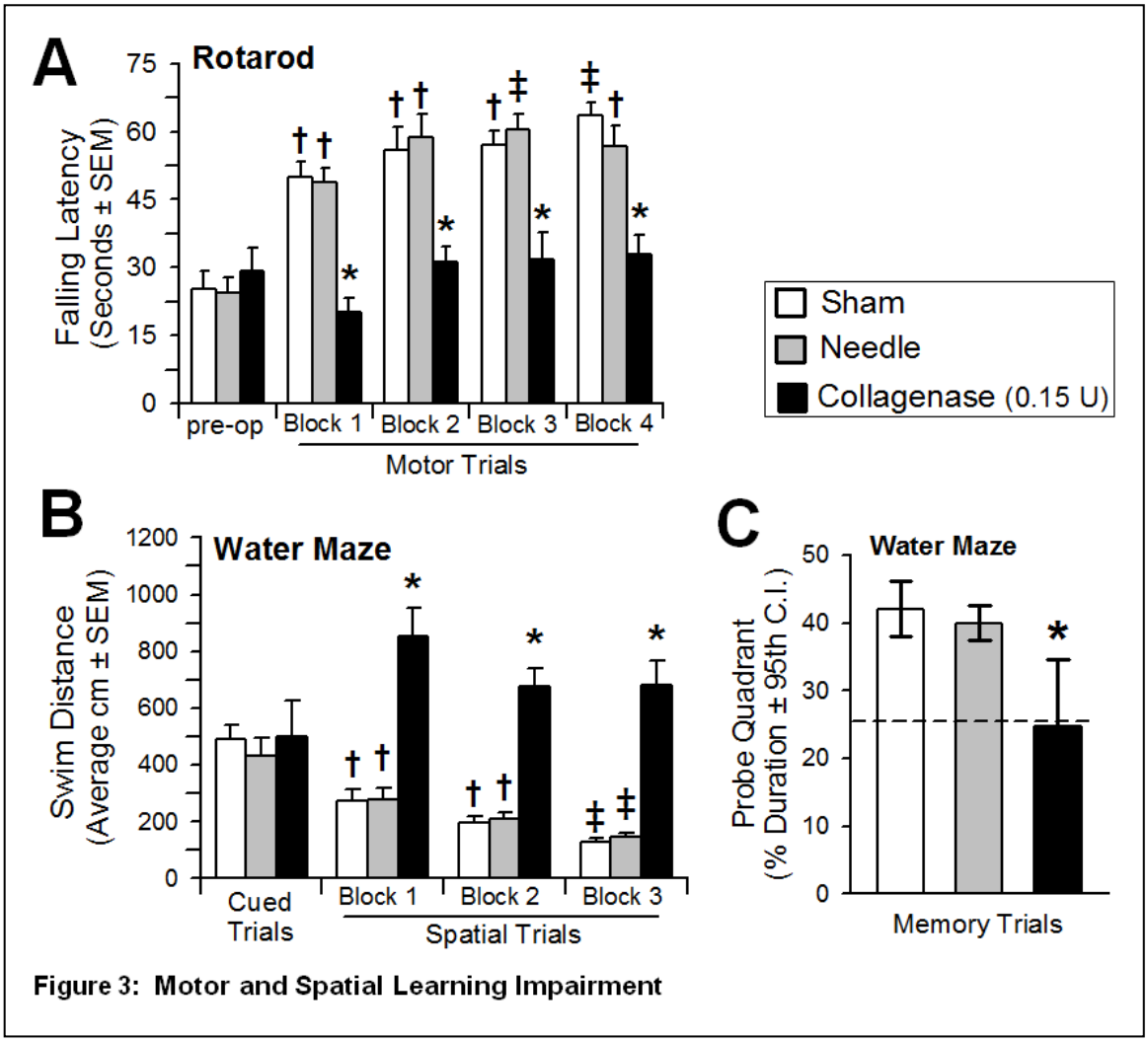

Figure 13. (A) Motor learning was assessed by the change in the latency to fall off an accelerating rotarod (2 rpm/ 5 sec) pre-operatively and across four daily blocks. (B) Spatial learning was assessed by the swim distance needed to find the visible (cued) versus the hidden (spatial) platforms in the water-maze. (C) Memory ability. Values expressed as mean ±SEM (rotarod, cued and spatial water-maze) and mean ±95th C.I. (probe quadrant), n=8 (per group), *P<0.05 compared with controls (sham and needle), †P<0.05 compared with pre-operation (rotarod) or cued trials (spatial water-maze), and ‡ P<0.05 compared with Block 1 (rotarod and spatial water-maze)

Table 4 Physiological Variables: Arterial Blood Gases (pH, PO_2, PCO_2), Mean Arterial Blood Pressure (BP), and Heart Rate (HR), during, and (30 Min, 24 Hr, 30 Days) after, Collagenase Infusion (C.I.)

Group	pH	PO_2 (mm Hg)	PCO_2 (mm Hg)	BP (mm Hg)	HR (per min)
During C.I.					
Sham	7.33±0.03	186±15	45±3	81±6	348±40
Needle	7.39±0.02	184±21	43±5	89±6	369±28
C.I.—0.15 Units	7.34±0.05	192±11	44±8	89±8	355±33
C.I.—0.3 Units	7.32±0.03	187±5	46±5	91±5	362±25
30 Min after C.I.					
Sham	7.32±0.01	185±20	48±5	84±6	347±48
Needle	7.38±0.05	186±14	44±3	88±8	359±14
C.I.—0.15 Units	7.30±0.08	188±10	48±9	88±10	351±33
C.I.—0.3 Units	7.29±0.03	173±17	50±9	90±5	380±37
24 Hr after C.I.					
Sham	7.50±0.04	192±12	36±5	84±5	348±20
Needle	7.52±0.02	181±7	37±7	78±3	361±17
C.I.—0.15 Units	7.47±0.03	188±11	38±4	85±9	359±34
C.I.—0.3 Units	7.38±0.06	179±14	49±9	90±9	329±46
30 Days after C.I.					
Sham	7.5±0.06	182±28	37±8	94±4	369±9
Needle	7.47±0.03	192±12	36±4	83±5	364±27
C.I.—0.15 Units	7.47±0.03	190±44	35±4	87±2	358±39

Values are mean ± SD. No significant differences among groups.

Results

Experimental Model of Pontine Hemorrhage

Systemic physiological variables were stable (see table 4) and all rats survived the surgical procedure. Within 30 minutes, the collagenase infused animals exhibited craniocaudal rotation, ataxic gait, cranial nerve deficit and limb dysfunction. 24 h pathological examinations demonstrated right caudal pontine hematomas surrounded with vasogenic edema, without subarachnoid, subdural or ventricular bleeding.

Hemostatic and Sensorimotor Characterization at 24 h

Unilateral collagenase infusion led to dose-dependent elevations of brain water, sensorimotor (composite neuroscore) deficit, hematoma volume, and vascular permeability ($P<0.05$, Figure 11A-D). Immunoblots show significant activation of MMP-2 and -9, and degradation of collagen-IV and ZO-1 ($P<0.05$, Figure 11E).

Functional Outcome over 30 Days

Infusion of collagenase (0.15 units) led to significant neurological (modified Garcia), locomotor (open field), and sensorimotor (wire suspension, beam balance, inclined plane) deficits ($P<0.05$, Figure 12A-E). Most parameters completely recovered by three weeks, however, the inclined plane performance did not improve ($P<0.05$, Figure 12E). Body weight did not differ between groups ($P>0.05$, Figure 12F).

Motor and Spatial Learning Assessment at 3 Weeks

Collagenase infused (0.15 units) animals performed significantly worse than controls across all post-operative rotarod (motor) testing blocks ($P<0.05$, Figure 13A) and were unable to improve upon their pre-operative performance ($P>0.05$), while, as expected, the controls performed better with subsequent blocks ($P<0.05$). For the water-maze, all groups performed the cued trials (place learning) without differences ($P>0.05$, Figure 13B). On spatial blocks, the collagenase infused (0.15 units) animals performed significantly worse than controls ($P<0.05$), and were unable to improve upon their cued trials ($P>0.05$). As expected, the controls performed better with subsequent blocks ($P<0.05$) and with the overall spatial probe (memory, Figure 13C).

Discussion

Application for Hemostatic Studies

Pontine hemorrhage (PH) is a poorly understood disease without an instructive model for experimental purposes (Lekic and Zhang, 2008). Hematomal growth is highly associated with worsened patient outcomes (Balci et al., 2005; Broderick et al., 1993; Dziewas et al., 2003; Goto et al., 1980; Wijdicks and St Louis, 1997). The control of hemostasis is therefore an important therapeutic approach (Steiner and Bosel, 2010), of which collagenase infusion is a mechanistic approach that is well suited (Foerch et al., 2008; Thiex et al., 2004). We therefore hypothesized that these mechanisms can be tested in this model, and our results stand in agreement with the findings by others concerning

brain edema, neurodeficit, hematoma volume, blood-brain barrier rupture, and MMP-2 and MMP-9 activation (Power et al., 2003; Rosenberg and Navratil, 1997; Wang and Tsirka, 2005). Since the higher dose (0.3 units of collagenase) produced a greater range of injury, compared to 0.15 units, we therefore chose the lower dose for long-term evaluations.

Importance of Neurocognitive Assessments

Up to half the survivors of pontine hemorrhage will have lasting and disabling sensorimotor and cognitive neurological deficits (Maeshima et al., 2010; Masiyama et al., 1985; Nys et al., 2007). Similar outcomes were achieved in this study using collagenase. Most neurological impairments resolved over the first three weeks, while motor-learning on the rotarod and cognitive ability on the water-maze remained impaired. The incomplete (inclined plane) hind-limb recovery is most likely rodent-specific due to the region of the pontine lesion, mapping to their hind-limb region (Peeters et al., 1999). Future studies with cytoprotective agents could target neurocognitive outcomes so that these patients may have a greater recovery some day.

In conclusion, we have characterized a highly reliable and easily reproducible experimental model of pontine hemorrhage using rats. This provides a basis for studying both the clinical and pathophysiological features of this disease, and establishes a foundation for performing further preclinical therapeutic investigations.

Acknowledgements

This study was partially supported by a grant (NS053407) from the National Institutes of Health to J.H.Z. The authors report no conflicts of interest.

CHAPTER FIVE

A NOVEL PRECLINICAL MODEL OF GERMINAL MATRIX HEMORRHAGE USING NEONATAL RATS

Abstract

Background: Germinal matrix hemorrhage (GMH) is a neurological disorder associated with very low birth weight premature infants. This event can lead to post-hemorrhagic hydrocephalus, cerebral palsy, and mental retardation. This study developed a novel animal model for pre-clinical investigations. Methods: Neonatal rats underwent infusion of clostridial collagenase into the right germinal matrix (anterior caudate) region using stereotaxic techniques. Developmental milestones were evaluated over ten-days, cognitive function at three weeks, and sensorimotor function at four weeks after collagenase infusion. This was accomplished by anthropometric quantifications of cranial, cerebral, cardiac and splenic growths. Results: Collagenase infusion led to delays in neonatal developmental milestones, followed by cognitive and sensorimotor dysfunctions in the juvenile animals. Cranial growth was accelerated during the first week after injury, and this was followed by significant brain atrophy, splenomegaly and cardiac hypertrophy three weeks later. Conclusion: This study characterized the developmental delays, mental retardation and cerebral palsy features resembling

the long-term clinical course after germinal matrix hemorrhage in premature infants. Pre-clinical testing of therapeutics in this experimental model could lead to improved patient outcomes, while expanding upon the pathophysiological understanding of this disease.

Introduction

Germinal matrix hemorrhage (GMH) is the rupture of immature blood vessels within the sub-ventricular (anterior caudate) progenitor cell region of neonatal brains (Ballabh, 2010) during the first 7 days of life (Kadri et al., 2006). GMH occurs in 20-25% of very low birth weight (VLBW ≤1500 grams) premature infants (Murphy et al., 2002; Vermont-Oxford, 1993; Vohr et al., 2000) and affects 3.5 per 1,000 births in the United States each year (Heron et al., 2010). This is an important clinical problem, since the consequences are hydrocephalus (post-hemorrhagic ventricular dilation), cognitive and motor developmental delay, cerebral palsy and mental retardation (Ballabh et al., 2004; Murphy et al., 2002). However, available animal models to study the pathophysiological basis of these outcomes is lacking (Balasubramaniam and Del Bigio, 2006). An important research priority is the development and validation of experimental models of brain hemorrhage for translational studies of human conditions (NINDS, 2005). Elevated MMP-2 and MMP-9 are associated with GMH induction in humans (Cockle et al., 2007; Schulz et al., 2004). Stereotaxic collagenase infusion is one the most commonly used methods in adult experimental intracerebral hemorrhage (ICH) studies (MacLellan et al., 2008; Rosenberg et al., 1990) and

functions as an MMP to lyse the extracellular-matrix around blood vessels to cause vascular rupture (Rosenberg et al., 1990; Yang et al., 1994). This approach enables investigations of neurological and brain injury outcomes (Andaluz et al., 2002; Foerch et al., 2008; Hartman et al., 2009; Lekic et al., 2010; MacLellan et al., 2008; Rosenberg et al., 1990; Thiex et al., 2004; Yang et al., 1994). In this study, we hypothesized that unilateral germinal-matrix collagenase infusion in neonatal rats would model features similar to clinical GMH (Ballabh et al., 2004; Murphy et al., 2002). With this approach, applications of therapeutic strategies can be tested to improve outcomes and to gain a better pathophysiological understanding of this disease (NINDS, 2005).

Methods and Materials

Animal Groups and General Procedures

This study was in accordance with the National Institutes of Health guidelines for the treatment of animals and was approved by the Institutional Animal Care and Use Committee at Loma Linda University. Timed pregnant Sprague-Dawley rats were housed with food and water available *ad libitum*. Postnatal day 7 (P7) pups were blindly assigned to the following (n= 8/ group): sham (naive), needle (control), and collagenase-infusion. All groups were evenly divided within each litter.

Experimental Model of GMH

Using aseptic technique, rat pups were gently anaesthetized with 3% isoflurane (in mixed air and oxygen) while placed prone onto a stereotaxic frame. Betadine sterilized the surgical scalp area, which was incised in the longitudinal plane to expose the skull and reveal the bregma. The following stereotactic coordinates were determined: 1 mm (anterior), 1.5 mm (lateral) and 3.5 mm (ventral) from bregma. A borehole (1 mm) was drilled, into which a 27 gauge needle was inserted at a rate of 1 mm/min. A microinfusion pump (Harvard Apparatus, Holliston, MA) infused 0.3 units of clostridial collagenase VII-S (Sigma, St Louis, MO) through a Hamilton syringe. The needle remained in place for an additional 10 min after injection to prevent “back-leakage”. After needle removal, the burr hole was sealed with bone wax, incision sutured closed, and the animals were allowed to recover. The entire surgery took on average 20 minutes. Upon recovering from anesthesia, the animals were returned to their dams. Needle-controls consisted of needle insertion alone without collagenase infusion, while naïve animals did not receive any surgery.

Developmental Milestones

Animals were assessed over 10 days after collagenase infusion. For the righting reflex, time needed for the rat pups to completely roll-over onto all four limbs after being placed on their backs was measured (Thullier et al., 1997). For negative geotaxis, the time needed for complete rotation (180°) after being

placed head down on a slope (20° angle), was recorded (Thullier et al., 1997). The maximum allotted time was 60 seconds per trial (2 trials/ day).

Cognitive Measures

Higher-order brain function was assessed during the third week after collagenase infusion. The T-Maze assessed short-term (working) memory (Hughes, 2004). Rats were placed into the stem (40 cm ×10 cm) of a maze and allowed to explore until one arm (46 cm × 10 cm) was chosen. From the sequence of ten trials, of left and right arm choices, the rate of spontaneous alternation (0% = none and 100% = complete, alternations/ trial) was calculated, as routinely performed (Fathali et al., 2010; Zhou et al., 2009). The Morris water-maze assessed spatial learning and memory on four daily blocks, as described previously in detail (Hartman et al., 2009; Lekic et al., 2010). The apparatus consisted of a metal pool (110cm diameter), filled to within 15cm of the upper edge, with a platform (11cm diameter) for the animal to escape onto, that changed location for each block (maximum= 60sec /trial), and digitally analyzed by Noldus Ethovision tracking software. Cued trials measured place learning with the escape platform visible above water. Spatial trials measured spatial learning with the platform submerged and probe trials measured spatial memory once the platform was removed. For the locomotor activity, in an open field, the path length in open-topped plastic boxes (49cm-long, 35.5cm-wide, 44.5cm-tall) was digitally recorded for 30 minutes and analyzed by Noldus Ethovision tracking software (Hartman et al., 2009).

Sensorimotor Outcome

At four weeks after collagenase infusion, animals were tested for functional ability. Neurodeficit was quantified using a summation of scores (maximum= 12), given for 1) postural reflex, 2) proprioceptive limb placing, 3) back pressure towards edge, 4) lateral pressure towards edge, 5) forelimb placement, and 6) lateral limb placement (2=severe, 1=moderate, 0=none), as routinely performed (Fathali et al., 2010). For the rotarod, striatal ability was assessed using an apparatus consisting of a horizontal, accelerated (2 rpm/ 5 sec), rotating cylinder (7cm-diameter x 9.5cm-wide), requiring continuous walking to avoid falling recorded by photobeam-circuit (Columbus Instruments) (Hartman et al., 2009; Lekic et al., 2010). For foot-fault, the number of complete limb missteps through the openings was counted over 2 minutes while exploring over an elevated wire (3 mm) grid (20 cm × 40 cm) floor (Zhou et al., 2009).

Assessment of Growth

Over 28 days after collagenase infusion, the head (width and height) and rump-to-crown (length) measurements were performed using a Boley Gauge (Franklin Dental Supply, Bellmore, NY), as previously described (Saad, 1990). Head-width was measured anterior to the side of ears, head-height from posterior the adjacent mandible, and rump-to-crown was the greatest cranial (caudal) to tail (rostral) extension. At the completion of experiments, the brains were removed, and hemispheres separated by midline incision (loss of brain weight has been used as the primary variable to estimate brain damage in

juvenile animals after neonatal brain injury (Andine et al., 1990)). For organ weights, the spleen and heart were separated from surrounding tissue and vessels. The quantification was performed using an analytical microbalance (model AE 100; Mettler Instrument Co., Columbus, OH) capable of 1.0μg precision.

Statistical Analysis

Significance was considered at $P<0.05$. Data was analyzed using analysis of variance (ANOVA), with repeated-measures (RM-ANOVA) for long-term neurobehavior. Significant interactions were explored with conservative Scheffe *post hoc* and Mann-Whitney rank sum when appropriate.

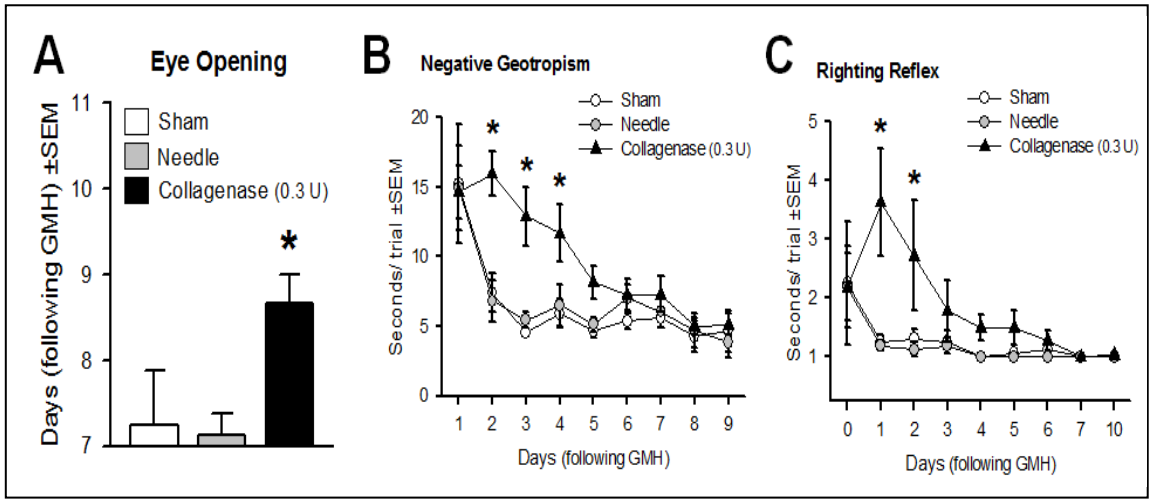

Figure 14. Developmental Delays: Neonates were assessed for: (A) Eye Opening latency, (B) Negative Geotropism, and (C) Righting Reflex, over ten days after collagenase infusion. Values expressed as mean ±SEM, n=8 (per group), **P*<0.05 compared with controls (sham and needle trauma)

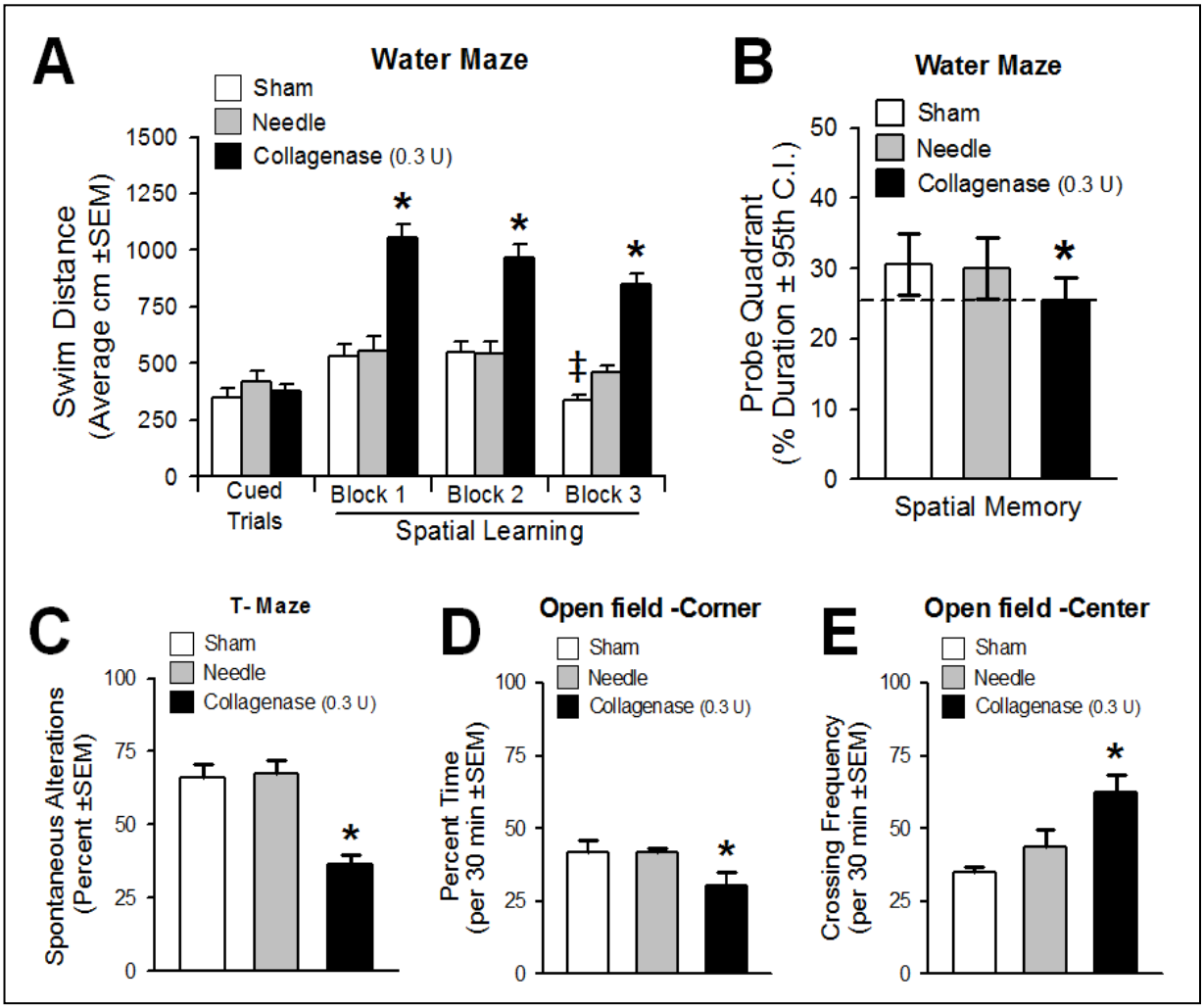

Figure 15. Cognitive Dysfunction: Higher-order function was measured at the third week after collagenase infusion. (A) Cued and Spatial Learning Water-maze, (B) Probe (Spatial Memory) Water-maze, (C) T-maze, (D) Open field (percent time in corner) and (E) Open field (center crossing frequency). Values expressed as mean ±95th C.I. (probe quadrant) or mean ±SEM (all others), n=8 (per group), *P<0.05 compared with controls (sham and needle trauma), and ‡ P<0.05 compared with Block 1 (spatial learning water-maze)

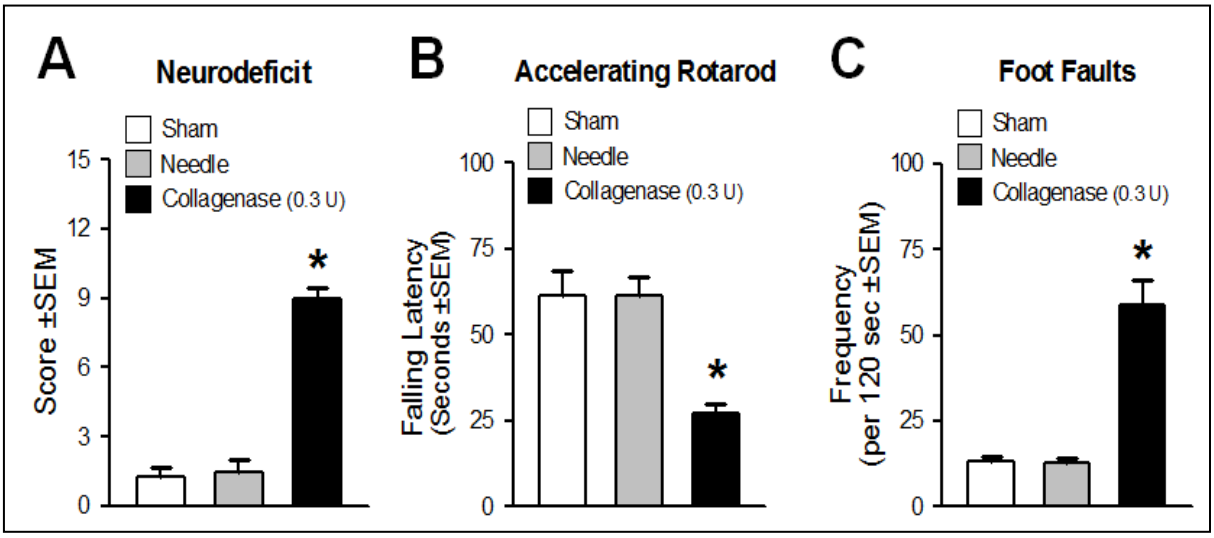

Figure 16. Sensorimotor Dysfunction: Cerebral palsy measurements were performed in the juveniles at one month after collagenase infusion: (A) Neurodeficit Score, (B) Rotarod and (C) Foot fault. Values expressed as mean ±SEM, n=8 (per group), *P<0.05 compared with controls (sham and needle trauma)

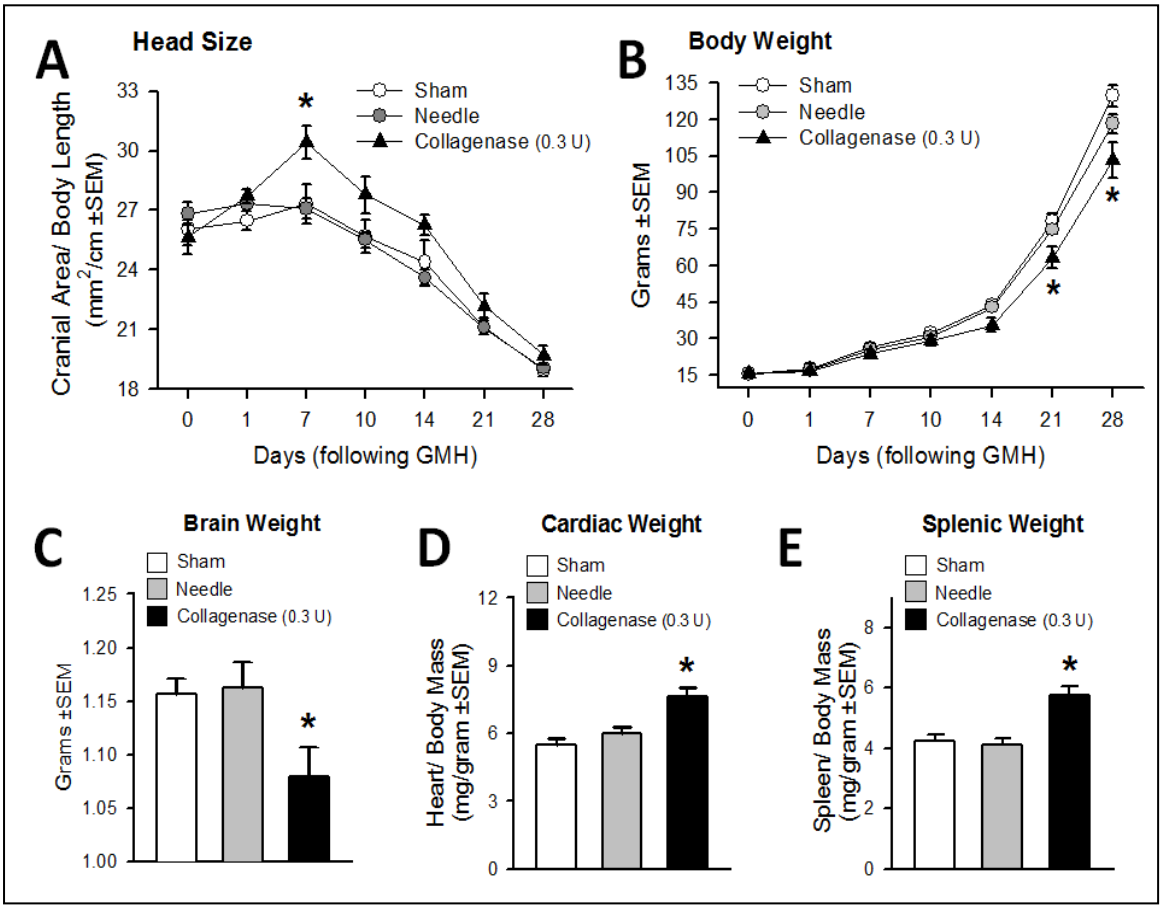

Figure 17. Cranial and Somatic Pediatric Growth: One month assessment of: (A) Head Size (Cranial Area/ Body Length), (B) Body Weight, (C) Brain Weight, (B) Cardiac Weight and (C) Splenic Weight. Values expressed as mean ±SEM, n=8 (per group), *P<0.05 compared with controls (sham and needle trauma)

Results

Collagenase infusion delayed the developmental acquisition of eye opening, negative geotropism and righting reflex by 2-3 days (Figures 14A-14C, $P<0.05$). Three weeks after GMH, significant deficits were discovered in spatial learning and memory (Figures 15A and 15B, $P<0.05$), T-maze (working) memory (Figure 15C, $P<0.05$), and hyperactivity, in the open field (decreased corner time and increased center crossings, Figures 15D and 15E, $P<0.05$). Juvenile animals had significant sensorimotor dysfunction, as revealed by the neurodeficit score, accelerating rotarod and foot fault (Figures 16A-16C, $P<0.05$). These dysfunctions were associated with increased cranial size at 7 days (Figure 17A, $P<0.05$), and dysfunctional growth of the body, brain, heart and spleen (Figures 17B-17E, $P<0.05$) three weeks later.

Discussion

Germinal matrix hemorrhage (GMH) is an important problem affecting approximately 12,000 births in the United States each year (Heron et al., 2010). The clinical consequences of GMH are developmental delay, cerebral palsy and mental retardation (Ballabh et al., 2004; Murphy et al., 2002). This study infused collagenase into the germinal matrix of neonatal rats as an approach to model these features, since animal models to study the basis of these outcomes is lacking (Balasubramaniam and Del Bigio, 2006).

This neonatal rat model of GMH resembles the neurological consequences seen in the pediatric population after hemorrhagic brain injury. Collagenase infusion led to developmental delays in the neonates that were followed by cognitive and sensorimotor dysfunction in the juvenile developmental stage. The cranium was enlarged compared to somatic growth during the first week, with significant brain atrophy, three weeks later. This presentation is likely a reflection of hydrocephalic cerebrospinal fluid build-up, leading to the cranial expansion and compression the brain tissue into an atrophic developmental growth pattern. Splenomegaly and cardiac-hypertrophy presented at one month after injury, and this could either be a reflection of the disproportionate somatic growth, or from prolonged peripheral hemostatic or inflammatory consequences to the brain bleed.

In summary, we have characterized a highly reliable and easily reproducible experimental model of germinal matrix hemorrhage using neonatal rats. This provides the basis for studying the clinical and pathophysiological features of this disease, and establishes a foundation for performing further preclinical therapeutic investigation.

Acknowledgements

This study was partially supported by a grant (NS053407) from the National Institutes of Health to J.H.Z. The authors report no conflicts of interest.

CHAPTER SIX

GENERAL DISCUSSION

Cerebellar Hemorrhage

For intracerebral hemorrhage, the control of hemostasis is related both to the therapeutic approaches,(Steiner and Bosel, 2010) and the propensity for injury through anticoagulant-use.(Prabhakaran et al., 2010) Epidemiological findings show that anticoagulant-associated ICH occurs more commonly at the cerebellum.(Flaherty et al., 2006) Since collagenase-induced ICH studies have evaluated hemostatic outcomes with clinically relevant anticoagulants (warfarin(Foerch et al., 2008) and tPA(Thiex et al., 2004)), we hypothesized these mechanisms are valid in this model as well. This hypothesis was tested, and found to stand in agreement with the findings by others concerning brain edema, neurodeficit, hematoma volume, blood-brain barrier rupture, and MMP-2 and MMP-9 activation.(Power et al., 2003; Rosenberg and Navratil, 1997; Wang and Tsirka, 2005) On the other hand, the lower dose (0.2 units of collagenase) failed to reproduce significant sensorimotor deficits at one day after injury.(MacLellan et al., 2008) Therefore, we chose 0.6 units of collagenase for the long-term studies. This is near to what was shown to avoid

neurotoxicity,(Matsushita et al., 2000) although this consideration is not a factor after cerebellar hemorrhage.(Qureshi et al., 2003)

Almost one-half of cerebellar hemorrhage survivors will retain deficits pertaining to motor-learning and visuospatial neurocognitive domains despite rehabilitation from ipsilateral losses of muscle tone, strength and coordination.(Baillieux et al., 2008; Dolderer et al., 2004; Kelly et al., 2001; Strick et al., 2009) Similar patterns were achieved in this study by using collagenase. Most neurological impairments resolved over the first three weeks, while motor-learning on the rotarod and cognitive ability on the water-maze remained impaired. The incomplete hind-limb (inclined plane) recovery is most likely rodent-specific due to the central placement of the cerebellar lesion, mapping to their hind-limb region, while the forelimbs are located more peripherally.(Peeters et al., 1999) Future studies with cytoprotective agents could target neurocognitive outcomes so that these patients may have greater recovery one day.

The cerebellum is organized into a geometric lattice with one-tenth the cerebral cortical volume, but four times the neuronal amount.(Andersen et al., 1992) Thirty days after collagenase infusion, we found a well circumscribed cystic-cavitary lesion within the right cerebellum. The atrophy was focal and did not affect the contralateral side, similar to basal ganglia hemorrhage using rats.(MacLellan et al., 2008) There also wasn't any difference between percent atrophy of the individual cerebellar layers; however, the early contralateral spreading of edema was followed by a bilateral loss in purkinje cell density one

month later. Since purkinje cells are the primary output of the cerebellum,(Baillieux et al., 2008) this could further augment neurocognitive deficits. All together, the neuronal tissue losses, present an appealing target for future neuroprotection.

In summary, we have characterized a highly reliable and easily reproducible experimental model of cerebellar hemorrhage using rats. This provides a basis for studying both the clinical and pathophysiological features of this disease, and establishes a foundation for performing further preclinical therapeutic investigations.

Postpartum Stroke

Intracerebral hemorrhage (ICH) is the least treatable form of stroke clinically, and is a devastating complication after pregnancy accompanied by life-long neurodeficits (Bateman et al., 2006; Broderick et al., 1999; Ciccone et al., 2008; Gebel and Broderick, 2000; Kittner et al., 1996; Skriver and Olsen, 1986). This study infused collagenase into the unilateral (right) side of the cerebellar hemisphere of postpartum rats, as an approach to model these features, since available animal models to study the pathophysiological basis of these outcomes is lacking.

Our results are in support of the clinical evidence for cerebral vascular vulnerability in the postpartum period. Around half the cases of ICH in this patient population will have the eclampsia (Sharshar et al., 1995), and this is related to hemostatically relevant increases of aquaporin-4 (AQP4) expression, blood-brain

barrier (BBB) disruption, and brain edema (Quick and Cipolla, 2005). In agreement, we found greater AQP4, and diminished COL-4 (collagen-IV) and ZO-1, expressions in the cerebella of postpartum female shams compared to the male controls. The collagenase model is an ideal method for study, since it did not alter these levels any further, however, the increased vascular vulnerability in postpartum animals, led to greater brain edema, neurodeficit, BBB-rupture and hematoma size across most doses studied. The lack of significant difference in cerebellar water at the highest collagenase dose (0.6 U) is likely either a reflection of mortality (i.e. severely injured animals died), or due to the high baseline AQP4 expressions leading to an edematous outflow.

In summary, we have characterized a highly reliable and easily reproducible experimental model of intracerebral hemorrhage using postpartum rats. Since the cerebellum contains some of the highest levels of AQP4 (Verkman, 2002) with the greatest AQP4 increase during the postpartum period (Wiegman et al., 2008), this ICH model provides a basis for studying the clinical and pathophysiological features of this disease, while establishing a foundation for performing further preclinical therapeutic investigations.

Pontine (brainstem) Hemorrhage

Pontine hemorrhage (PH) is a poorly understood disease without an instructive model for experimental purposes (Lekic and Zhang, 2008). Hematomal growth is highly associated with worsened patient outcomes (Balci et al., 2005; Broderick et al., 1993; Dziewas et al., 2003; Goto et al., 1980; Wijdicks

and St Louis, 1997). The control of hemostasis is therefore an important therapeutic approach (Steiner and Bosel, 2010), of which collagenase infusion is a mechanistic approach that is well suited (Foerch et al., 2008; Thiex et al., 2004). We therefore hypothesized that these mechanisms can be tested in this model, and our results stand in agreement with the findings by others concerning brain edema, neurodeficit, hematoma volume, blood-brain barrier rupture, and MMP-2 and MMP-9 activation (Power et al., 2003; Rosenberg and Navratil, 1997; Wang and Tsirka, 2005). Since the higher dose (0.3 units of collagenase) produced a greater range of injury, compared to 0.15 units, we therefore chose the lower dose for long-term evaluations.

Up to half the survivors of pontine hemorrhage will have lasting and disabling sensorimotor and cognitive neurological deficits (Maeshima et al., 2010; Masiyama et al., 1985; Nys et al., 2007). Similar outcomes were achieved in this study using collagenase. Most neurological impairments resolved over the first three weeks, while motor-learning on the rotarod and cognitive ability on the water-maze remained impaired. The incomplete (inclined plane) hind-limb recovery is most likely rodent-specific due to the region of the pontine lesion, mapping to their hind-limb region (Peeters et al., 1999). Future studies with cytoprotective agents could target neurocognitive outcomes so that these patients may have a greater recovery some day.

In summary, we have characterized a highly reliable and easily reproducible experimental model of pontine hemorrhage using rats. This provides a basis for studying both the clinical and pathophysiological features of this

disease, and establishes a foundation for performing further preclinical therapeutic investigations.

Germinal Matrix (Intraventricular) Neonatal Hemorrhage

Germinal matrix hemorrhage (GMH) is an important problem affecting approximately 12,000 births in the United States each year (Heron et al., 2010). The clinical consequences of GMH are developmental delay, cerebral palsy and mental retardation (Ballabh et al., 2004; Murphy et al., 2002). This study infused collagenase into the germinal matrix of neonatal rats as an approach to model these features, since animal models to study the basis of these outcomes is lacking (Balasubramaniam and Del Bigio, 2006).

This neonatal rat model of GMH resembles the neurological consequences seen in the pediatric population after hemorrhagic brain injury. Collagenase infusion led to developmental delays in the neonates that were followed by cognitive and sensorimotor dysfunction in the juvenile developmental stage. The cranium was enlarged compared to somatic growth during the first week, with significant brain atrophy, three weeks later. This presentation is likely a reflection of hydrocephalic cerebrospinal fluid build-up, leading to the cranial expansion and compression the brain tissue into an atrophic developmental growth pattern. Splenomegaly and cardiac-hypertrophy presented at one month after injury, and this could either be a reflection of the disproportionate somatic growth, or from prolonged peripheral hemostatic or inflammatory consequences to the brain bleed.

In summary, we have characterized a highly reliable and easily reproducible experimental model of germinal matrix hemorrhage using neonatal rats. This provides the basis for studying the clinical and pathophysiological features of this disease, and establishes a foundation for performing further preclinical therapeutic investigation.

Conclusion

The hindbrain has many critical neural tracts and nuclei involved in processing and transmitting information between the cerebral cortexes and spine. Furthermore, injury to this area can be particularly devastating. This brain region may have less innate neurovascular protective mechanisms, and greater amount of cell death and injury in comparison to supratentorial strokes. A very limited, yet significant amount of experimental study has been done for ischemic posterior circulation stroke, while hemorrhage into the infratentorium has received no study to date. In spite of shared mechanisms between ischemic and hemorrhagic strokes, there is an urgent need to study ICH in the hindbrain. Future studies can use these new models of ICH, and an array of other ischemic models, to test interventions for reversing the mechanisms of injury in this brain region.

The post-partum state reverses the cytoprotective effects commonly associated with the female gender, and this leads to greater brain injury and worsened neurological function after cerebellar hemorrhage. This model can be

used to test future treatment strategies after ICH, and to better understand the mechanistic basis for brain injury in this important patient population.

Germinal matrix hemorrhage is an important neurological problem associated with prematurity. Pre-clinical animal models need to be developed to study this condition further. This experimental model mimics the clinical situation well, and further translational investigations can be applied to test treatment strategies.

REFERENCES

1. 1989. Vascular malformations in the brainstem. Lancet 2**,** 720-721.

2. Adeoye, O., Woo, D., Haverbusch, M., Sekar, P., Moomaw, C. J., Broderick, J., and Flaherty, M. L., 2008. Surgical management and case-fatality rates of intracerebral hemorrhage in 1988 and 2005. Neurosurgery 63**,** 1113-1117; discussion 1117-1118.

3. Andaluz, N., Zuccarello, M., and Wagner, K. R., 2002. Experimental animal models of intracerebral hemorrhage. Neurosurg Clin N Am 13**,** 385-393.

4. Andersen, B. B., Korbo, L., and Pakkenberg, B., 1992. A quantitative study of the human cerebellum with unbiased stereological techniques. J Comp Neurol 326**,** 549-560.

5. Andine, P., Thordstein, M., Kjellmer, I., Nordborg, C., Thiringer, K., Wennberg, E., and Hagberg, H., 1990. Evaluation of brain damage in a rat model of neonatal hypoxic-ischemia. J Neurosci Methods 35**,** 253-260.

6. Atlas, S. W., and Thulbom, K. R., 2002. Intracranial Hemorrhage, Magnetic Resonance Imaging of the Brain Lippincott Williams & Wilkins, Philadelphia, pp. 773-832.

7. Atlas, S. W., and Thulborn, K. R., 1998. MR detection of hyperacute parenchymal hemorrhage of the brain. AJNR Am J Neuroradiol 19**,** 1471-1477.

8. Back, T., 1998. Pathophysiology of the ischemic penumbra--revision of a concept. Cell Mol Neurobiol 18**,** 621-638.

9. Baillieux, H., De Smet, H. J., Paquier, P. F., De Deyn, P. P., and Marien, P., 2008. Cerebellar neurocognition: insights into the bottom of the brain. Clin Neurol Neurosurg 110**,** 763-773.

10. Balasubramaniam, J., and Del Bigio, M. R., 2006. Animal models of germinal matrix hemorrhage. J Child Neurol 21**,** 365-371.

11. Balci, K., Asil, T., Kerimoglu, M., Celik, Y., and Utku, U., 2005. Clinical and neuroradiological predictors of mortality in patients with primary pontine hemorrhage. Clin Neurol Neurosurg 108**,** 36-39.

12. Ballabh, P., 2010. Intraventricular hemorrhage in premature infants: mechanism of disease. Pediatr Res 67**,** 1-8.

13. Ballabh, P., Braun, A., and Nedergaard, M., 2004. The blood-brain barrier: an overview: structure, regulation, and clinical implications. Neurobiol Dis 16**,** 1-13.

14. Bamford, J., Sandercock, P., Dennis, M., Burn, J., and Warlow, C., 1991. Classification and natural history of clinically identifiable subtypes of cerebral infarction. Lancet 337**,** 1521-1526.

15. Bateman, B. T., Schumacher, H. C., Bushnell, C. D., Pile-Spellman, J., Simpson, L. L., Sacco, R. L., and Berman, M. F., 2006. Intracerebral hemorrhage in pregnancy: frequency, risk factors, and outcome. Neurology 67**,** 424-429.

16. Belayev, L., Obenaus, A., Zhao, W., Saul, I., Busto, R., Wu, C., Vigdorchik, A., Lin, B., and Ginsberg, M. D., 2007. Experimental intracerebral hematoma in the rat: characterization by sequential magnetic resonance imaging, behavior, and histopathology. Effect of albumin therapy. Brain Res 1157**,** 146-155.

17. Bergui, M., Cerrato, P., and Bradac, G. B., 2007. Stroke attributable to acute basilar occlusion. Curr Treat Options Neurol 9**,** 126-135.

18. Bogousslavsky, J., Van Melle, G., and Regli, F., 1988. The Lausanne Stroke Registry: analysis of 1,000 consecutive patients with first stroke. Stroke 19**,** 1083-1092.

19. Bradley, W. G., Jr., 1993. MR appearance of hemorrhage in the brain. Radiology 189**,** 15-26.

20. Bristow, M. S., Simon, J. E., Brown, R. A., Eliasziw, M., Hill, M. D., Coutts, S. B., Frayne, R., Demchuk, A. M., and Mitchell, J. R., 2005. MR perfusion and diffusion in acute ischemic stroke: human gray and white matter have different thresholds for infarction. J Cereb Blood Flow Metab 25**,** 1280-1287.

21. Broderick, J., Connolly, S., Feldmann, E., Hanley, D., Kase, C., Krieger, D., Mayberg, M., Morgenstern, L., Ogilvy, C. S., Vespa, P., and Zuccarello, M., 2007. Guidelines for the management of spontaneous intracerebral hemorrhage in adults: 2007 update: a guideline from the American Heart Association/American Stroke Association Stroke Council, High Blood Pressure Research Council, and the Quality of Care and Outcomes in Research Interdisciplinary Working Group. Stroke 38**,** 2001-2023.

22. Broderick, J. P., Adams, H. P., Jr., Barsan, W., Feinberg, W., Feldmann, E., Grotta, J., Kase, C., Krieger, D., Mayberg, M., Tilley, B., Zabramski, J. M., and Zuccarello, M., 1999. Guidelines for the management of spontaneous intracerebral hemorrhage: A statement for healthcare professionals from a special writing group of the Stroke Council, American Heart Association. Stroke 30**,** 905-915.

23. Broderick, J. P., Brott, T. G., Duldner, J. E., Tomsick, T., and Huster, G., 1993. Volume of intracerebral hemorrhage. A powerful and easy-to-use predictor of 30-day mortality. Stroke 24**,** 987-993.

24. Burns, J., Lisak, R., Schut, L., and Silberberg, D., 1980. Recovery following brainstem hemorrhage. Ann Neurol 7**,** 183-184.

25. Chaturvedi, S., Lukovits, T. G., Chen, W., and Gorelick, P. B., 1999. Ischemia in the territory of a hypoplastic vertebrobasilar system. Neurology 52**,** 980-983.

26. Choudhri, T. F., Hoh, B. L., Solomon, R. A., Connolly, E. S., Jr., and Pinsky, D. J., 1997. Use of a spectrophotometric hemoglobin assay to objectively quantify intracerebral hemorrhage in mice. Stroke 28**,** 2296-2302.

27. Choy, M., Ganesan, V., Thomas, D. L., Thornton, J. S., Proctor, E., King, M. D., van der Weerd, L., Gadian, D. G., and Lythgoe, M. F., 2006. The chronic vascular and haemodynamic response after permanent bilateral common carotid occlusion in newborn and adult rats. J Cereb Blood Flow Metab 26**,** 1066-1075.

28. Chung, C. S., and Park, C. H., 1992. Primary pontine hemorrhage: a new CT classification. Neurology 42**,** 830-834.

29. Chung, Y., and Haines, S. J., 1993. Experimental brain stem surgery. Neurosurg Clin N Am 4**,** 405-414.

30. Ciccone, A., Pozzi, M., Motto, C., Tiraboschi, P., and Sterzi, R., 2008. Epidemiological, clinical, and therapeutic aspects of primary intracerebral hemorrhage. Neurol Sci 29 Suppl 2**,** S256-257.

31. Cipolla, M. J., McCall, A. L., Lessov, N., and Porter, J. M., 1997. Reperfusion decreases myogenic reactivity and alters middle cerebral artery function after focal cerebral ischemia in rats. Stroke 28**,** 176-180.

32. Clark, W. M., Albers, G. W., Madden, K. P., and Hamilton, S., 2000. The rtPA (alteplase) 0- to 6-hour acute stroke trial, part A (A0276g) : results of a double-blind, placebo-controlled, multicenter study. Thromblytic therapy in acute ischemic stroke study investigators. Stroke 31**,** 811-816.

33. Clark, W. M., Wissman, S., Albers, G. W., Jhamandas, J. H., Madden, K. P., and Hamilton, S., 1999. Recombinant tissue-type plasminogen activator (Alteplase) for ischemic stroke 3 to 5 hours after symptom onset. The ATLANTIS Study: a randomized controlled trial. Alteplase Thrombolysis for Acute Noninterventional Therapy in Ischemic Stroke. JAMA 282**,** 2019-2026.

34. Cockle, J. V., Gopichandran, N., Walker, J. J., Levene, M. I., and Orsi, N. M., 2007. Matrix metalloproteinases and their tissue inhibitors in preterm perinatal complications. Reprod Sci 14**,** 629-645.

35. Colombel, C., Lalonde, R., and Caston, J., 2002. The effects of unilateral removal of the cerebellar hemispheres on motor functions and weight gain in rats. Brain Res 950**,** 231-238.

36. Cossu, M., Dorcaratto, A., Pau, A., Rodriguez, G., Sehrbundt Viale, E., Siccardi, D., and Viale, G. L., 1991. Changes in infratentorial blood flow following experimental cerebellar haemorrhage. A preliminary report. Ital J Neurol Sci 12**,** 69-73.

37. Cossu, M., Pau, A., Siccardi, D., and Viale, G. L., 1994. Infratentorial ischaemia following experimental cerebellar haemorrhage in the rat. Acta Neurochir (Wien) 131**,** 146-150.

38. Dawson, S. L., Blake, M. J., Panerai, R. B., and Potter, J. F., 2000. Dynamic but not static cerebral autoregulation is impaired in acute ischaemic stroke. Cerebrovasc Dis 10**,** 126-132.

39. Dawson, S. L., Panerai, R. B., and Potter, J. F., 2003. Serial changes in static and dynamic cerebral autoregulation after acute ischaemic stroke. Cerebrovasc Dis 16**,** 69-75.

40. de Bray, J. M., Tranquart, F., Saumet, J. L., Berson, M., and Pourcelot, L., 1994. Cerebral vasodilation capacity: acute intracranial hypertension and supra- and infra-tentorial artery velocity recording. Clin Physiol 14**,** 501-512.

41. de Oliveira, E., Tedeschi, H., Rhoton, A., and Peace, D., 1995. Microsurgical anatomy of the posterior circulation: vertebral and basilar arteries. In: Carter, L., Spetzler, R., and Hamilton, M., (Eds.), Neurovascular Surgery. McGraw-Hill Inc., New York, pp. 25-34.

42. Diedler, J., Sykora, M., Rupp, A., Poli, S., Karpel-Massler, G., Sakowitz, O., and Steiner, T., 2009. Impaired cerebral vasomotor activity in spontaneous intracerebral hemorrhage. Stroke 40**,** 815-819.

43. Dohmen, C., Bosche, B., Graf, R., Reithmeier, T., Ernestus, R. I., Brinker, G., Sobesky, J., and Heiss, W. D., 2007. Identification and clinical impact of impaired cerebrovascular autoregulation in patients with malignant middle cerebral artery infarction. Stroke 38**,** 56-61.

44. Dolderer, S., Kallenberg, K., Aschoff, A., Schwab, S., and Schwarz, S., 2004. Long-term outcome after spontaneous cerebellar haemorrhage. Eur Neurol 52**,** 112-119.

45. Donnan, G. A., 1992. Investigation of patients with stroke and transient ischaemic attacks. Lancet 339**,** 473-477.

46. Donnelly, D. F., Jiang, C., and Haddad, G. G., 1992. Comparative responses of brain stem and hippocampal neurons to O2 deprivation: in vitro intracellular studies. Am J Physiol 262**,** L549-554.

47. Drummond, J. C., Oh, Y. S., Cole, D. J., and Shapiro, H. M., 1989. Phenylephrine-induced hypertension reduces ischemia following middle cerebral artery occlusion in rats. Stroke 20**,** 1538-1544.

48. Duvemoy, H., 1999. Human Brain Stem Vessels. Springer, Berlin.

49. Dziewas, R., Kremer, M., Ludemann, P., Nabavi, D. G., Drager, B., and Ringelstein, B., 2003. The prognostic impact of clinical and CT parameters in patients with pontine hemorrhage. Cerebrovasc Dis 16**,** 224-229.

50. Eames, P. J., Blake, M. J., Dawson, S. L., Panerai, R. B., and Potter, J. F., 2002. Dynamic cerebral autoregulation and beat to beat blood pressure control are impaired in acute ischaemic stroke. J Neurol Neurosurg Psychiatry 72**,** 467-472.

51. Facchinetti, F., Dawson, V. L., and Dawson, T. M., 1998. Free radicals as mediators of neuronal injury. Cell Mol Neurobiol 18**,** 667-682.

52. Fathali, N., Ostrowski, R. P., Lekic, T., Jadhav, V., Tong, W., Tang, J., and Zhang, J. H., 2010. Cyclooxygenase-2 inhibition provides lasting protection against neonatal hypoxic-ischemic brain injury. Crit Care Med 38**,** 572-578.

53. Felberg, R. A., Grotta, J. C., Shirzadi, A. L., Strong, R., Narayana, P., Hill-Felberg, S. J., and Aronowski, J., 2002. Cell death in experimental intracerebral hemorrhage: the "black hole" model of hemorrhagic damage. Ann Neurol 51**,** 517-524.

54. Ferbert, A., Bruckmann, H., and Drummen, R., 1990. Clinical features of proven basilar artery occlusion. Stroke 21**,** 1135-1142.

55. Fernandez, A. M., de la Vega, A. G., and Torres-Aleman, I., 1998. Insulin-like growth factor I restores motor coordination in a rat model of cerebellar ataxia. Proc Natl Acad Sci U S A 95**,** 1253-1258.

56. Fewel, M. E., Thompson, B. G., Jr., and Hoff, J. T., 2003. Spontaneous intracerebral hemorrhage: a review. Neurosurg Focus 15**,** E1.

57. Flaherty, M. L., Haverbusch, M., Sekar, P., Kissela, B., Kleindorfer, D., Moomaw, C. J., Sauerbeck, L., Schneider, A., Broderick, J. P., and Woo, D., 2006. Long-term mortality after intracerebral hemorrhage. Neurology 66**,** 1182-1186.

58. Flaherty, M. L., Haverbusch, M., Sekar, P., Kissela, B. M., Kleindorfer, D., Moomaw, C. J., Broderick, J. P., and Woo, D., 2006. Location and outcome of anticoagulant-associated intracerebral hemorrhage. Neurocrit Care 5**,** 197-201.

59. Flaherty, M. L., Woo, D., Haverbusch, M., Sekar, P., Khoury, J., Sauerbeck, L., Moomaw, C. J., Schneider, A., Kissela, B., Kleindorfer, D., and Broderick, J. P., 2005. Racial variations in location and risk of intracerebral hemorrhage. Stroke 36**,** 934-937.

60. Foerch, C., Arai, K., Jin, G., Park, K. P., Pallast, S., van Leyen, K., and Lo, E. H., 2008. Experimental model of warfarin-associated intracerebral hemorrhage. Stroke 39**,** 3397-3404.

61. Foulkes, M. A., Wolf, P. A., Price, T. R., Mohr, J. P., and Hier, D. B., 1988. The Stroke Data Bank: design, methods, and baseline characteristics. Stroke 19**,** 547-554.

62. Fujiwara, N., Higashi, H., Shimoji, K., and Yoshimura, M., 1987. Effects of hypoxia on rat hippocampal neurones in vitro. J Physiol 384**,** 131-151.

63. Ganesan, V., Chong, W. K., Cox, T. C., Chawda, S. J., Prengler, M., and Kirkham, F. J., 2002. Posterior circulation stroke in childhood: risk factors and recurrence. Neurology 59**,** 1552-1556.

64. Garbin, L., Habetswallner, F., and Clivati, A., 1997. Vascular reactivity in middle cerebral artery and basilar artery by transcranial Doppler in normals subjects during hypoxia. Ital J Neurol Sci 18**,** 135-137.

65. Gebel, J. M., and Broderick, J. P., 2000. Intracerebral hemorrhage. Neurol Clin 18**,** 419-438.

66. Glass, T. A., Hennessey, P. M., Pazdera, L., Chang, H. M., Wityk, R. J., Dewitt, L. D., Pessin, M. S., and Caplan, L. R., 2002. Outcome at 30 days

in the New England Medical Center Posterior Circulation Registry. Arch Neurol 59, 369-376.

67. Gong, Y., Hua, Y., Keep, R. F., Hoff, J. T., and Xi, G., 2004. Intracerebral hemorrhage: effects of aging on brain edema and neurological deficits. Stroke 35, 2571-2575.

68. Goto, N., Kaneko, M., Hosaka, Y., and Koga, H., 1980. Primary pontine hemorrhage: clinicopathological correlations. Stroke 11, 84-90.

69. Greer, D. M., Koroshetz, W. J., Cullen, S., Gonzalez, R. G., and Lev, M. H., 2004. Magnetic resonance imaging improves detection of intracerebral hemorrhage over computed tomography after intra-arterial thrombolysis. Stroke 35, 491-495.

70. Haacke, E. M., Cheng, N. Y., House, M. J., Liu, Q., Neelavalli, J., Ogg, R. J., Khan, A., Ayaz, M., Kirsch, W., and Obenaus, A., 2005. Imaging iron stores in the brain using magnetic resonance imaging. Magn Reson Imaging 23, 1-25.

71. Haacke, M. E., Herigault, G., Yu, Y., Kido, D., Tong, K., Obenaus, A., and Reichenbach, J. R., 2002. Observing Tumor Vascularity Noninvasively Using Magnetic Resonance Imaging. Image Anal Stereol 21, 107-113.

72. Hacke, W., Kaste, M., Fieschi, C., Toni, D., Lesaffre, E., von Kummer, R., Boysen, G., Bluhmki, E., Hoxter, G., Mahagne, M. H., and et al., 1995. Intravenous thrombolysis with recombinant tissue plasminogen activator for acute hemispheric stroke. The European Cooperative Acute Stroke Study (ECASS). JAMA 274, 1017-1025.

73. Haque, T. L., Miki, Y., Kanagaki, M., Takahashi, T., Yamamoto, A., Konishi, J., Nozaki, K., and Hashimoto, N., 2003. MR contrast of ferritin and hemosiderin in the brain: comparison among gradient-echo, conventional spin-echo and fast spin-echo sequences. Eur J Radiol 48, 230-236.

74. Hartman, R., Lekic, T., Rojas, H., Tang, J., and Zhang, J. H., 2009. Assessing functional outcomes following intracerebral hemorrhage in rats. Brain Res 1280, 148-157.

75. Hata, R., Matsumoto, M., Hatakeyama, T., Ohtsuki, T., Handa, N., Niinobe, M., Mikoshiba, K., Sakaki, S., Nishimura, T., Yanagihara, T., and et al., 1993. Differential vulnerability in the hindbrain neurons and local cerebral blood flow during bilateral vertebral occlusion in gerbils. Neuroscience 56, 423-439.

76. Hemphill, J. C., 3rd, Bonovich, D. C., Besmertis, L., Manley, G. T., and Johnston, S. C., 2001. The ICH score: a simple, reliable grading scale for intracerebral hemorrhage. Stroke 32**,** 891-897.

77. Hermier, M., and Nighoghossian, N., 2004. Contribution of susceptibility-weighted imaging to acute stroke assessment. Stroke 35**,** 1989-1994.

78. Heron, M., Sutton, P. D., Xu, J., Ventura, S. J., Strobino, D. M., and Guyer, B., 2010. Annual summary of vital statistics: 2007. Pediatrics 125**,** 4-15.

79. Hida, W., Kikuchi, Y., Okabe, S., Miki, H., Kurosawa, H., and Shirato, K., 1996. CO2 response for the brain stem artery blood flow velocity in man. Respir Physiol 104**,** 71-75.

80. Hill, M. D., and Silver, F. L., 2001. Epidemiologic predictors of 30-day survival in cerebellar hemorrhage. J Stroke Cerebrovasc Dis 10**,** 118-121.

81. Hill, M. D., Silver, F. L., Austin, P. C., and Tu, J. V., 2000. Rate of stroke recurrence in patients with primary intracerebral hemorrhage. Stroke 31**,** 123-127.

82. Hua, Y., Nakamura, T., Keep, R. F., Wu, J., Schallert, T., Hoff, J. T., and Xi, G., 2006. Long-term effects of experimental intracerebral hemorrhage: the role of iron. J Neurosurg 104**,** 305-312.

83. Hua, Y., Schallert, T., Keep, R. F., Wu, J., Hoff, J. T., and Xi, G., 2002. Behavioral tests after intracerebral hemorrhage in the rat. Stroke 33**,** 2478-2484.

84. Hughes, R. N., 2004. The value of spontaneous alternation behavior (SAB) as a test of retention in pharmacological investigations of memory. Neurosci Biobehav Rev 28**,** 497-505.

85. Ito, H., Yokoyama, I., Iida, H., Kinoshita, T., Hatazawa, J., Shimosegawa, E., Okudera, T., and Kanno, I., 2000. Regional differences in cerebral vascular response to PaCO2 changes in humans measured by positron emission tomography. J Cereb Blood Flow Metab 20**,** 1264-1270.

86. Jaramillo, A., Gongora-Rivera, F., Labreuche, J., Hauw, J. J., and Amarenco, P., 2006. Predictors for malignant middle cerebral artery infarctions: a postmortem analysis. Neurology 66**,** 815-820.

87. Jensen, M. B., and St Louis, E. K., 2005. Management of acute cerebellar stroke. Arch Neurol 62**,** 537-544.

88. Kadri, H., Mawla, A. A., and Kazah, J., 2006. The incidence, timing, and predisposing factors of germinal matrix and intraventricular hemorrhage (GMH/IVH) in preterm neonates. Childs Nerv Syst 22**,** 1086-1090.

89. Kelly, P. J., Stein, J., Shafqat, S., Eskey, C., Doherty, D., Chang, Y., Kurina, A., and Furie, K. L., 2001. Functional recovery after rehabilitation for cerebellar stroke. Stroke 32**,** 530-534.

90. Kety, S. S., and Schmidt, C. F., 1948. The Effects of Altered Arterial Tensions of Carbon Dioxide and Oxygen on Cerebral Blood Flow and Cerebral Oxygen Consumption of Normal Young Men. J Clin Invest 27**,** 484-492.

91. Kittner, S. J., Stern, B. J., Feeser, B. R., Hebel, R., Nagey, D. A., Buchholz, D. W., Earley, C. J., Johnson, C. J., Macko, R. F., Sloan, M. A., Wityk, R. J., and Wozniak, M. A., 1996. Pregnancy and the risk of stroke. N Engl J Med 335**,** 768-774.

92. Korbo, L., Andersen, B. B., Ladefoged, O., and Moller, A., 1993. Total numbers of various cell types in rat cerebellar cortex estimated using an unbiased stereological method. Brain Res 609**,** 262-268.

93. Kushner, M. J., and Bressman, S. B., 1985. The clinical manifestations of pontine hemorrhage. Neurology 35**,** 637-643.

94. Leggio, M. G., Molinari, M., Neri, P., Graziano, A., Mandolesi, L., and Petrosini, L., 2000. Representation of actions in rats: the role of cerebellum in learning spatial performances by observation. Proc Natl Acad Sci U S A 97**,** 2320-2325.

95. Lekic, T., Hartman, R., Rojas, H., Manaenko, A., Chen, W., Ayer, R., Tang, J., and Zhang, J. H., 2010. Protective effect of melatonin upon neuropathology, striatal function, and memory ability after intracerebral hemorrhage in rats. J Neurotrauma 27**,** 627-637.

96. Lekic, T., Tang, J., and Zhang, J. H., 2008. Rat model of intracerebellar hemorrhage. Acta Neurochir Suppl 105**,** 131-134.

97. Lekic, T., and Zhang, J. H., 2008. Posterior circulation stroke and animal models. Front Biosci 13**,** 1827-1844.

98. Lindsberg, P. J., and Mattle, H. P., 2006. Therapy of basilar artery occlusion: a systematic analysis comparing intra-arterial and intravenous thrombolysis. Stroke 37**,** 922-928.

99. Lister, J. R., Rhoton, A. L., Jr., Matsushima, T., and Peace, D. A., 1982. Microsurgical anatomy of the posterior inferior cerebellar artery. Neurosurgery 10**,** 170-199.

100. MacLellan, C. L., Silasi, G., Poon, C. C., Edmundson, C. L., Buist, R., Peeling, J., and Colbourne, F., 2008. Intracerebral hemorrhage models in rat: comparing collagenase to blood infusion. J Cereb Blood Flow Metab 28**,** 516-525.

101. Macleod, M., 2006. Current issues in the treatment of acute posterior circulation stroke. CNS Drugs 20**,** 611-621.

102. Macleod, M. R., Davis, S. M., Mitchell, P. J., Gerraty, R. P., Fitt, G., Hankey, G. J., Stewart-Wynne, E. G., Rosen, D., McNeil, J. J., Bladin, C. F., Chambers, B. R., Herkes, G. K., Young, D., and Donnan, G. A., 2005. Results of a multicentre, randomised controlled trial of intra-arterial urokinase in the treatment of acute posterior circulation ischaemic stroke. Cerebrovasc Dis 20**,** 12-17.

103. Maeshima, S., Osawa, A., and Kunishio, K., 2010. Cognitive dysfunction in a patient with brainstem hemorrhage. Neurol Sci.

104. Masiyama, S., Niizuma, H., and Suzuki, J., 1985. Pontine haemorrhage: a clinical analysis of 26 cases. J Neurol Neurosurg Psychiatry 48**,** 658-662.

105. Matsumoto, S., Kuwabara, S., and Moritake, K., 2000. Effects of cerebrovascular autoregulation and CO2 reactivity in experimental localized brainstem infarction. Neurol Res 22**,** 197-203.

106. Matsushita, K., Meng, W., Wang, X., Asahi, M., Asahi, K., Moskowitz, M. A., and Lo, E. H., 2000. Evidence for apoptosis after intercerebral hemorrhage in rat striatum. J Cereb Blood Flow Metab 20**,** 396-404.

107. Mendelow, A. D., Gregson, B. A., Fernandes, H. M., Murray, G. D., Teasdale, G. M., Hope, D. T., Karimi, A., Shaw, M. D., and Barer, D. H., 2005. Early surgery versus initial conservative treatment in patients with spontaneous supratentorial intracerebral haematomas in the International Surgical Trial in Intracerebral Haemorrhage (STICH): a randomised trial. Lancet 365**,** 387-397.

108. Mendelow, A. D., and Unterberg, A., 2007. Surgical treatment of intracerebral haemorrhage. Curr Opin Crit Care 13**,** 169-174.

109. Merzeau, S., Preckel, M. P., Fromy, B., Leftheriotis, G., and Saumet, J. L., 2000. Differences between cerebral and cerebellar autoregulation during progressive hypotension in rats. Neurosci Lett 280**,** 103-106.

110. Morioka, J., Fujii, M., Kato, S., Fujisawa, H., Akimura, T., Suzuki, M., and Kobayashi, S., 2006. Surgery for spontaneous intracerebral hemorrhage has greater remedial value than conservative therapy. Surg Neurol 65**,** 67-72; discussion 72-63.

111. Murphy, B. P., Inder, T. E., Rooks, V., Taylor, G. A., Anderson, N. J., Mogridge, N., Horwood, L. J., and Volpe, J. J., 2002. Posthaemorrhagic ventricular dilatation in the premature infant: natural history and predictors of outcome. Arch Dis Child Fetal Neonatal Ed 87**,** F37-41.

112. NINDS, 2005. Priorities for clinical research in intracerebral hemorrhage: report from a National Institute of Neurological Disorders and Stroke workshop. Stroke 36**,** e23-41.

113. Nys, G. M., van Zandvoort, M. J., de Kort, P. L., Jansen, B. P., de Haan, E. H., and Kappelle, L. J., 2007. Cognitive disorders in acute stroke: prevalence and clinical determinants. Cerebrovasc Dis 23**,** 408-416.

114. O'Reilly, J. P., Jiang, C., and Haddad, G. G., 1995. Major differences in response to graded hypoxia between hypoglossal and neocortical neurons. Brain Res 683**,** 179-186.

115. Occhiogrosso, G., Edgar, M. A., Sandberg, D. I., and Souweidane, M. M., 2003. Prolonged convection-enhanced delivery into the rat brainstem. Neurosurgery 52**,** 388-393; discussion 393-384.

116. Okauchi, M., Hua, Y., Keep, R. F., Morgenstern, L. B., and Xi, G., 2009. Effects of deferoxamine on intracerebral hemorrhage-induced brain injury in aged rats. Stroke 40**,** 1858-1863.

117. Olah, L., Franke, C., Schwindt, W., and Hoehn, M., 2000. CO(2) reactivity measured by perfusion MRI during transient focal cerebral ischemia in rats. Stroke 31**,** 2236-2244.

118. Oorschot, D. E., 1996. Total number of neurons in the neostriatal, pallidal, subthalamic, and substantia nigral nuclei of the rat basal ganglia: a stereological study using the cavalieri and optical disector methods. J Comp Neurol 366**,** 580-599.

119. Payne, H. A., Maravilla, K. R., Levinstone, A., Heuter, J., and Tindall, R. S., 1978. Recovery from primary pontine hemorrhage. Ann Neurol 4**,** 557-558.

120. Peeters, R. R., Verhoye, M., Vos, B. P., Van Dyck, D., Van Der Linden, A., and De Schutter, E., 1999. A patchy horizontal organization of the somatosensory activation of the rat cerebellum demonstrated by functional MRI. Eur J Neurosci 11**,** 2720-2730.

121. Power, C., Henry, S., Del Bigio, M. R., Larsen, P. H., Corbett, D., Imai, Y., Yong, V. W., and Peeling, J., 2003. Intracerebral hemorrhage induces macrophage activation and matrix metalloproteinases. Ann Neurol 53**,** 731-742.

122. Prabhakaran, S., Rivolta, J., Vieira, J. R., Rincon, F., Stillman, J., Marshall, R. S., and Chong, J. Y., 2010. Symptomatic Intracerebral Hemorrhage Among Eligible Warfarin-Treated Patients Receiving Intravenous Tissue Plasminogen Activator for Acute Ischemic Stroke. Arch Neurol.

123. Quick, A. M., and Cipolla, M. J., 2005. Pregnancy-induced up-regulation of aquaporin-4 protein in brain and its role in eclampsia. FASEB J 19**,** 170-175.

124. Qureshi, A. I., Mendelow, A. D., and Hanley, D. F., 2009. Intracerebral haemorrhage. Lancet 373**,** 1632-1644.

125. Qureshi, A. I., Suri, M. F., Ostrow, P. T., Kim, S. H., Ali, Z., Shatla, A. A., Guterman, L. R., and Hopkins, L. N., 2003. Apoptosis as a form of cell death in intracerebral hemorrhage. Neurosurgery 52**,** 1041-1047; discussion 1047-1048.

126. Qureshi, A. I., Tuhrim, S., Broderick, J. P., Batjer, H. H., Hondo, H., and Hanley, D. F., 2001. Spontaneous intracerebral hemorrhage. N Engl J Med 344**,** 1450-1460.

127. Reinhard, M., Waldkircher, Z., Timmer, J., Weiller, C., and Hetzel, A., 2008. Cerebellar autoregulation dynamics in humans. J Cereb Blood Flow Metab 28**,** 1605-1612.

128. Rosenberg, G. A., and Kaufman, D. M., 1976. Cerebellar hemorrhage: reliability of clinical evaluation. Stroke 7**,** 332-336.

129. Rosenberg, G. A., Mun-Bryce, S., Wesley, M., and Kornfeld, M., 1990. Collagenase-induced intracerebral hemorrhage in rats. Stroke 21**,** 801-807.

130. Rosenberg, G. A., and Navratil, M., 1997. Metalloproteinase inhibition blocks edema in intracerebral hemorrhage in the rat. Neurology 48**,** 921-926.

131. Saad, A. Y., 1990. Postnatal effects of nicotine on incisor development of albino mouse. J Oral Pathol Med 19**,** 426-429.

132. Saria, A., and Lundberg, J. M., 1983. Evans blue fluorescence: quantitative and morphological evaluation of vascular permeability in animal tissues. J Neurosci Methods 8**,** 41-49.

133. Sato, M., Pawlik, G., and Heiss, W. D., 1984. Comparative studies of regional CNS blood flow autoregulation and responses to CO2 in the cat. Effects of altering arterial blood pressure and PaCO2 on rCBF of cerebrum, cerebellum, and spinal cord. Stroke 15**,** 91-97.

134. Schmidt, W. M., Kraus, C., Hoger, H., Hochmeister, S., Oberndorfer, F., Branka, M., Bingemann, S., Lassmann, H., Muller, M., Macedo-Souza, L. I., Vainzof, M., Zatz, M., Reis, A., and Bittner, R. E., 2007. Mutation in the Scyl1 gene encoding amino-terminal kinase-like protein causes a recessive form of spinocerebellar neurodegeneration. EMBO Rep 8**,** 691-697.

135. Schomer, D. F., Marks, M. P., Steinberg, G. K., Johnstone, I. M., Boothroyd, D. B., Ross, M. R., Pelc, N. J., and Enzmann, D. R., 1994. The anatomy of the posterior communicating artery as a risk factor for ischemic cerebral infarction. N Engl J Med 330**,** 1565-1570.

136. Schulz, C. G., Sawicki, G., Lemke, R. P., Roeten, B. M., Schulz, R., and Cheung, P. Y., 2004. MMP-2 and MMP-9 and their tissue inhibitors in the plasma of preterm and term neonates. Pediatr Res 55**,** 794-801.

137. Schwarz, S., Georgiadis, D., Aschoff, A., and Schwab, S., 2002. Effects of body position on intracranial pressure and cerebral perfusion in patients with large hemispheric stroke. Stroke 33**,** 497-501.

138. Scorziello, A., Pellegrini, C., Forte, L., Tortiglione, A., Gioielli, A., Iossa, S., Amoroso, S., Tufano, R., Di Renzo, G., and Annunziato, L., 2001. Differential vulnerability of cortical and cerebellar neurons in primary culture to oxygen glucose deprivation followed by reoxygenation. J Neurosci Res 63**,** 20-26.

139. Sharshar, T., Lamy, C., and Mas, J. L., 1995. Incidence and causes of strokes associated with pregnancy and puerperium. A study in public hospitals of Ile de France. Stroke in Pregnancy Study Group. Stroke 26**,** 930-936.

140. Shimamura, N., Matchett, G., Yatsushige, H., Calvert, J. W., Ohkuma, H., and Zhang, J., 2006. Inhibition of integrin alphavbeta3 ameliorates focal cerebral ischemic damage in the rat middle cerebral artery occlusion model. Stroke 37**,** 1902-1909.

141. Shiokawa, O., Sadoshima, S., Fujii, K., Yao, H., and Fujishima, M., 1988. Impairment of cerebellar blood flow autoregulation during cerebral ischemia in spontaneously hypertensive rats. Stroke 19**,** 615-622.

142. Shiokawa, O., Sadoshima, S., Kusuda, K., Nishimura, Y., Ibayashi, S., and Fujishima, M., 1986. Cerebral and cerebellar blood flow autoregulations in acutely induced cerebral ischemia in spontaneously hypertensive rats--transtentorial remote effect. Stroke 17**,** 1309-1313.

143. Skriver, E. B., and Olsen, T. S., 1986. Tissue damage at computed tomography following resolution of intracerebral hematomas. Acta Radiol Diagn (Stockh) 27**,** 495-500.

144. Song, S., Hua, Y., Keep, R. F., Hoff, J. T., and Xi, G., 2007. A new hippocampal model for examining intracerebral hemorrhage-related neuronal death: effects of deferoxamine on hemoglobin-induced neuronal death. Stroke 38**,** 2861-2863.

145. St Louis, E. K., Wijdicks, E. F., and Li, H., 1998. Predicting neurologic deterioration in patients with cerebellar hematomas. Neurology 51**,** 1364-1369.

146. Steinberg, G. K., Drake, C. G., and Peerless, S. J., 1993. Deliberate basilar or vertebral artery occlusion in the treatment of intracranial aneurysms. Immediate results and long-term outcome in 201 patients. J Neurosurg 79**,** 161-173.

147. Steiner, T., and Bosel, J., 2010. Options to restrict hematoma expansion after spontaneous intracerebral hemorrhage. Stroke 41**,** 402-409.

148. Strick, P. L., Dum, R. P., and Fiez, J. A., 2009. Cerebellum and nonmotor function. Annu Rev Neurosci 32**,** 413-434.

149. Sung, L., Shibata, M., Eskew, J. D., Shipulina, N., Morales, P. J., and Smith, A., 2000. Cell-surface events for metallothionein-1 and heme oxygenase-1 regulation by the hemopexin-heme transport system. Antioxid Redox Signal 2**,** 753-765.

150. Sutherland, G. R., and Auer, R. N., 2006. Primary intracerebral hemorrhage. J Clin Neurosci 13**,** 511-517.

151. Tang, J., Liu, J., Zhou, C., Alexander, J. S., Nanda, A., Granger, D. N., and Zhang, J. H., 2004. Mmp-9 deficiency enhances collagenase-induced intracerebral hemorrhage and brain injury in mutant mice. J Cereb Blood Flow Metab 24**,** 1133-1145.

152. Thach, W. T., 1996. On the specific role of the cerebellum in motor learning and cognition: Clues from PET activation and lesion studies in man. Behav. Brain Sci. 19**,** 411-431.

153. Thiex, R., Mayfrank, L., Rohde, V., Gilsbach, J. M., and Tsirka, S. A., 2004. The role of endogenous versus exogenous tPA on edema formation in murine ICH. Exp Neurol 189**,** 25-32.

154. Thullier, F., Lalonde, R., Cousin, X., and Lestienne, F., 1997. Neurobehavioral evaluation of lurcher mutant mice during ontogeny. Brain Res Dev Brain Res 100**,** 22-28.

155. Timmann, D., Konczak, J., Ilg, W., Donchin, O., Hermsdorfer, J., Gizewski, E. R., and Schoch, B., 2009. Current advances in lesion-symptom mapping of the human cerebellum. Neuroscience 162**,** 836-851.

156. Tong, K. A., Ashwal, S., Holshouser, B. A., Nickerson, J. P., Wall, C. J., Shutter, L. A., Osterdock, R. J., Haacke, E. M., and Kido, D., 2004. Diffuse axonal injury in children: clinical correlation with hemorrhagic lesions. Ann Neurol 56**,** 36-50.

157. Tuhrim, S., 2008. Intracerebral hemorrhage--improving outcome by reducing volume? N Engl J Med 358**,** 2174-2176.

158. Verkman, A. S., 2002. Physiological importance of aquaporin water channels. Ann Med 34**,** 192-200.

159. Vermont-Oxford, 1993. The Vermont-Oxford Trials Network: very low birth weight outcomes for 1990. Investigators of the Vermont-Oxford Trials Network Database Project. Pediatrics 91**,** 540-545.

160. Voetsch, B., DeWitt, L. D., Pessin, M. S., and Caplan, L. R., 2004. Basilar artery occlusive disease in the New England Medical Center Posterior Circulation Registry. Arch Neurol 61**,** 496-504.

161. Vohr, B. R., Wright, L. L., Dusick, A. M., Mele, L., Verter, J., Steichen, J. J., Simon, N. P., Wilson, D. C., Broyles, S., Bauer, C. R., Delaney-Black, V., Yolton, K. A., Fleisher, B. E., Papile, L. A., and Kaplan, M. D., 2000. Neurodevelopmental and functional outcomes of extremely low birth weight infants in the National Institute of Child Health and Human Development Neonatal Research Network, 1993-1994. Pediatrics 105**,** 1216-1226.

162. Wagner, K. R., Sharp, F. R., Ardizzone, T. D., Lu, A., and Clark, J. F., 2003. Heme and iron metabolism: role in cerebral hemorrhage. J Cereb Blood Flow Metab 23**,** 629-652.

163. Wang, J., and Tsirka, S. E., 2005. Neuroprotection by inhibition of matrix metalloproteinases in a mouse model of intracerebral haemorrhage. Brain 128**,** 1622-1633.

164. Wiegman, M. J., Bullinger, L. V., Kohlmeyer, M. M., Hunter, T. C., and Cipolla, M. J., 2008. Regional expression of aquaporin 1, 4, and 9 in the brain during pregnancy. Reprod Sci 15**,** 506-516.

165. Wijdicks, E. F., and St Louis, E., 1997. Clinical profiles predictive of outcome in pontine hemorrhage. Neurology 49**,** 1342-1346.

166. Worthley, L. I., and Holt, A. W., 2000. Acute ischaemic stroke: part II. The vertebrobasilar circulation. Crit Care Resusc 2**,** 140-145.

167. Wycliffe, N. D., Choe, J., Holshouser, B., Oyoyo, U. E., Haacke, E. M., and Kido, D. K., 2004. Reliability in detection of hemorrhage in acute stroke by a new three-dimensional gradient recalled echo susceptibility-weighted imaging technique compared to computed tomography: a retrospective study. J Magn Reson Imaging 20**,** 372-377.

168. Xi, G., Keep, R. F., and Hoff, J. T., 2006. Mechanisms of brain injury after intracerebral haemorrhage. Lancet Neurol 5**,** 53-63.

169. Yang, G. Y., Betz, A. L., Chenevert, T. L., Brunberg, J. A., and Hoff, J. T., 1994. Experimental intracerebral hemorrhage: relationship between brain edema, blood flow, and blood-brain barrier permeability in rats. J Neurosurg 81**,** 93-102.

170. Zhou, Y., Fathali, N., Lekic, T., Tang, J., and Zhang, J. H., 2009. Glibenclamide improves neurological function in neonatal hypoxia-ischemia in rats. Brain Res 1270**,** 131-139.

171. Zia, E., Engstrom, G., Svensson, P. J., Norrving, B., and Pessah-Rasmussen, H., 2009. Three-year survival and stroke recurrence rates in patients with primary intracerebral hemorrhage. Stroke 40**,** 3567-3573.

172. Zuccarello, M., Fiore, D. L., Trincia, G., De Caro, R., Pardatscher, K., and Andrioli, G. C., 1983. Traumatic primary brain stem haemorrhage. A clinical and experimental study. Acta Neurochir (Wien) 67**,** 103-113.